CHARLES UNIVERSITY IN PRAGUE

FACULTY OF SCIENCE

Study programme: Biology

Branch of study: Genetics, Molecular Biology and Virology

Monika Burócziová

Molecular characteristics of mismatch repair pathway in ovarian cancer

Molekulární charakteristika mismatch reparační dráhy u ovariálního karcinomu

Master's Thesis

Supervisor: Pavel Vodička, M.D., Ph.D.

Prague, 2016

Declaration

I herewith declare that I have produced this Diploma thesis without the prohibited assistance of third parties and without making use of aids other than those specified; notions taken over directly or indirectly from other sources have been identified as such. This Thesis has not previously been presented in identical or similar form to any other Czech or foreign examination board.

The thesis work was conducted from 2012 to 2016 under the supervision of Pavel Vodička, M.D., Ph.D. at the Institute Experimental medicine, ASCR, v.v.i.

Prohlášení

Prohlašuji, že jsem závěrečnou práci zpracovala samostatně a že jsem uvedla všechny použité informační zdroje a literaturu. Tato práce ani její podstatná část nebyla předložena k získání jiného nebo stejného akademického titulu.

V Praze, 01.05. 2016 Podpis

Acknowledgements

I would like to express my gratitude to those who gave me the possibility to complete this thesis. Thank to Pavel Vodička, M.D. CS.c. for his enthusiastic supervision, guidance and support throughout the duration of this project.
Also, I would like to thank to Ľudmila Vodičková M.D. Ph.D., Radka Václavíková Ph.D. and Kateřina Elsnerová, MS.c for productive discussions, I acknowledge the immense help and assistance with project. I would like to thank to Radka Václavíková Ph.D. and prof. Lukáš Rob, M.D. CS.c. for providing biological material for presented thesis.
I am indebted to Valéria Grobárová, Ph.D. for healthy critical point of view.
Finally, I would like to thank those closest to me, to my family and my sister Judita for unconditional support.

The thesis was supported by grants: IGA: **NT14056** Molekulární a genetické biomarkery v patogenesi a resistenci karcinomu ovaria and IGA: **NT 14329** Hodnocení významu změn molekulárně-biologických faktorů v prognóze generalizace radikálně operovaného kolorektálního karcinomu

Abstract

In humans, multi enzymatic processes are involved in maintaining DNA stability and cellular homeostasis. Cells undergo several episodes to survive and protect itself in daily basis. Accumulation of DNA errors and breaks are repaired by dynamic machinery, such as mismatch repair (MMR), replication-related process.

In presented diploma thesis, we report the studied MMR pathway and its involvement in malignancy of epithelial ovarian cancer (EOC). Our working hypothesis postulated that core genes of MMR, such as *MLH1* and *MSH2* are down-regulated in malignant cells. Cells therefore become incapable to repair accumulating DNA damage, undergo apoptosis or most likely uncontrolled proliferation. Above mentioned genes may also be silenced in cancer patients at transcription, translation or epigenetic levels.

Our aims were to clarify and to investigate the importance of MMR based on mRNA transcription, protein stability and promoter hypermethylation on a set of major MMR genes, particularly *MLH1, MSH2, PMS1, MLH3, MSH6, MSH3,* and *PMS2*.

In our study, we analysed samples from 63 epithelial ovarian cancer patients and 12 non-malignant reference tissues using RT-qPCR, MS-HRM, and Western Blotting methods. Consequently, our results show down-regulation of all MMR genes except for *MSH2* (up-regulated) in tumor tissues as compared to reference tissues. By comparing clinical data (stages I+II vs. III+IV), *MLH1* and *PMS1* were significantly up -regulated in stages III+IV (*MLH1* $P \leq 0,017$; *PMS1* $P \leq 0,042$), *MSH2* in stages I+II ($P \leq 0.033$). The regulatory link between promoter methylation and mRNA down-regulation was not observed, since none of the tested tumor tissue sample exhibited enhanced methylation status. The *in vitro* studies showed significant G_2 arrest in *MLH1* deficient cell line after neocarzinostatin mediated DNA damage.

Taking together, these results suggest that regulation of MMR pathway in ovarian tumors might be correlated with microsatellite instability (MSI), miRNA regulation, or other endo-exogenous stress induced pathways.

Keywords: mismatch repair, ovarian carcinoma, MLH1, MS-HRM

Abstrakt

Udržování stability genomu a buněčné homeostázy je v lidském organismu zajišťováno mnohaúrovňovými a mnohačetnými enzymatickými ději. Buňky se musí každodenně vypořádat s řadou událostí, při kterých dochází k poškození DNA, s cílem přežití a udržení integrity genetické informace (DNA). Nahromaděné chyby ve struktuře DNA a zlomy DNA jsou opravované pomocí dynamického aparátu, jako je například dráha opravy nesprávně přiřazených nukleotidů (MMR).

V předkládané diplomové práci byla studována MMR dráha a její podíl na malignizaci epiteliální rakoviny vaječníků (EOC). Pracovní hypotéza byla, že exprese hlavních genů MMR dráhy, jako jsou *MLH1* a *MSH2*, je v rakovinných buňkách utlumena. Tyto buňky jsou pak neschopny opravit nahromaděné chyby v DNA, což vede buď k apoptóze nebo s vyšší pravděpodobností k jejich nekontrolovanému pomnožení. Dále byl podroben testování předpoklad, že výše zmiňované geny jsou utlumeny u pacientek trpících EOC rakovinou na transkripční, translační nebo epigenetické úrovni.

Cílem práce bylo objasnit a prozkoumat význam MMR dráhy na utlumení exprese mRNA, nestabilitě proteinů a hypermetylaci promotorů skupiny hlavních genů MMR dráhy, a to konkrétně u *MLH1*, *MSH2*, *PMS1*, *MLH3*, *MSH6*, *MSH3* a *PMS2*.

V rámci studie bylo analyzováno 63 vzorků EOC a 12 zdravých vaječníků pomocí metod RT-qPCR, MS-HRM a Western blotu. Výsledky ukazují na útlum exprese u všech sledovaných genů MMR dráhy vyjma *MSH2*, kde exprese byla zvýšena ve srovnání se zdravou tkání. Pokud vztáhneme sledované změny na klinická data a porovnáme stádium I a II se stádii III a IV, exprese *MLH1* a *PMS1* byla významně zvýšena u stádií III a IV, (MLH1 $p \leq 0{,}017$; PMS1 $p \leq 0{,}042$) a exprese *MSH2* ve stádiu I a II ($p \leq 0{,}033$). Vzájemný vztah mezi metylací promotoru a poklesem hladiny mRNA nebyl pozorován. U žádně zesledovaných pacientek nebyla naměřena zvýšená metylace v promotorových oblastech MMR genů.

In vitro studie vyjevily významný nárůst G_2 zástavy buněčného cyklu u buněk s chybějícím *MLH1* po podání neocarzinostatinu, jež vede ke vzniku DNA poškození.

Obdržené výsledky souhrně naznačují, že regulace MMR dráhy u nádorů vaječníků může souviset s nestabilitou mikrosatelitů (MSI), regulací miRNA, nebo s jinými stresovými dráhami vnějšího a/nebo vnitřního původu.

Klíčova slova: mismatch opravy, ovariální karcinom, MLH1, MS-HRM

Contents

Abbreviations

18S	ribosomal RNA
9-1-1	Rad9-Rad1-Hus1 complex; cell-cycle checkpoint response complex
ACTB	beta-actin; highly conserved protein that is involved in cell motility, structure, and integrity
Alt-EJ	alternative end joining
Artemis	an essential factor of recombination in the repair of DNA double-strand breaks and non-homologous end joining
ASCR	the Academy of Science Czech Republic
ATM	ataxia telangiectasia mutated; serine-protein kinase; which activates checkpoint
ATP	adenosine triphosphate
ATPase	an enzyme that catalyses the formation of ATP from ADP
ATR	ataxia telangiectasia and Rad3-related protein; serine/threonine-protein kinase
B2M	Beta-2-Microglobulin
BER	base excision repair
BRAF	B-Raf proto-oncogene, serine/threonine kinase
BRCA1	breast cancer type 1 susceptibility protein; E3 ubiquitin-protein ligase that plays a important role in DNA repair
BRCA2	tumor suppressor proteins; involved in DNA repair
BrdU	bromodeoxyuridine; the thymidine analog that incorporating into newly synthetized DNA, S-phase idicator
C	cytosine
CA-125	cancer antigen 125; surface protein found on ovarian tumor cells; tumor marker
CDC25	Cdc25 family of phosphatases; dephosphorylate inhibitory Tyr and Thr residues on cyclin-dependent kinases
Cdk	mammalian cyclin-dependent kinases; cyclin-dependent kinases (CDKs) are activated by the binding to a cyclin
Chk1	serine/threonine-protein kinase; required for checkpoint mediated cell cycle arrest in response to DNA damage
Chk2	serine/threonine-protein kinase; regulates cell cycle checkpoints and apoptosis in response to DNA damage
c-NHEJ	Classical non-homologous end joining

C_t	cycle threshold; defined as the number of cycles required for the fluorescent signal to cross the threshold
CtIP	CtBP-interacting protein, DNA endonuclease, cooperates with the MRN complex and processing mitotic double-strand breaks
DAPI	4',6-Diamidino-2-Phenylindole, blue-fluorescent DNA stain used for cell viability assessment
DBSs	DNA double strand breaks
DDR	DNA Damage Response Pathways
DNA polymerase III	the enzyme that performs the 5'-3' polymerase function
DNA	deoxiribonucleic acid
DNA-PK	DNA-dependent protein kinase; serine/threonine-protein kinase; involved in DNA non-homologous end joining (NHEJ) required for double-strand break (DSB) repair
DSB(s)	DNA double-strand break(s)
EFG	epidermal growth factor; a potent mitogenic factor that plays an important role in the growth, proliferation
EOC	epithelial ovarian cancer
EXO1	exonuclease I; EXO1 cooperates with MSH2, involved in mismatch repair and recombination
FACS	fluorescence-activated cell sorting
FEN1	Flap Structure-Specific Endonuclease 1; removes 5' overhanging flaps in DNA repair and processes the 5' ends of Okazaki fragments
FSC-A	forward scatter–area
FSC-H	forward scatter–height plotted against FSC-A (area) to gate singlets
G1	cell cycle growth phase 1
G2	cell cycle growth phase 2
GAPDH	glyceraldehyde-3-phosphate dehydrogenase; has glyceraldehyde-3-phosphate dehydrogenase and nitrosylase activities; plays a role in glycolysis and nuclear functions
gDNA	genomic DNA
GATC	bacterial GATC sequences
geNORM	an algorithm to determine the most stable reference genes for qPCR application
GFP	green fluorescent protein
GG-NER	global genome NER sub-pathway
GUS	ß-Glucuronidase; internal control for gene expression analysis
H2A	a type of histone; a part of nucleosome core particle

H2AX	histone that replaces conventional H2A in a subset of nucleosomes
HNPCC	hereditary nonpolyposis colorectal cancer; hereditary cancer syndrome; result of defective mismatch repair proteins
HPRT	hypoxanthine phosphoribosyltransferase 1; a transferase, which catalyses conversion of hypoxanthine to inosine and guanine to guanosine monophosphate; reference gene
HR	homologous recombination
HRP	Horseradish Peroxidase; enzyme used in immunoblotting; used as the reporter enzyme for SuperSignal-Chemiluminescent substrates
HUS1	checkpoint protein; component of the 9-1-1 cell-cycle checkpoint response complex, involved in DNA repair
IKK-ß	protein plays role in activation of NF-κB; phosphorylates NF-κB inhibitor
Ki67	proliferation marker, Ki-67 protein is associated with cell proliferation
KRAS	Kirsten rat sarcoma viral oncogene homolog; a member of the small GTPase;
Ku70/80	heterodimer that is a main component of the non-homologous end-joining pathway that repairs DNA double-strand breaks
Ligase I	ATP-dependent DNA ligase
Ligase III	ATP-dependent DNA ligase
LRP	long-patch repair; sub-pathway of base excision repair
MCF7	human breast adenocarcinoma cell line
MCM9	minichromosome maintenance 9 homologous recombination repair factor; essential protein for replication initiation; binding to chromatin and recruiting he MCM2-7 helicase to replication origins
miRNA	microRNA; small non-protein coding RNA about 21-25 nucleotides in length; regulating gene expression by directly targeting mRNAs
MLH1	mutL homolog 1; plays a central role in DNA mismatch repair
MLH3	MutL Homolog 3; is a member of the MutL-homolog family of DNA mismatch repair genes
MMR	mismatch repair
MRE11	meiotic recombination 11; double-strand break repair protein; component of the MRN complex, which plays a central role in double-strand break (DSB) repair, DNA recombination
MRN	heterotrimeric protein complex consisting of Mre11, Rad50 and Nbs1
mRNA	messenger ribonucleic acid

MSH2	mutS homolog 2; DNA mismatch repair protein
MSH6	mutS homolog 6; DNA mismatch repair protein
MS-HRM	methylation-sensitive high resolution melting; an approach for estimating promoter methylation
MSI	microsatellite instability
MSI-H	microsatellite instability-high
MSI-L	microsatellite instability-low
MutL	component of mismatch repair complex in *E. coli*, physicaly interacts with MutS; stimulates the loading of helicase II
MutLγ	forming heterodimeric (MLH1/MLH3) protein complexes
MutSα	forming heterodimeric MSH2/MSH6, component of mismatch repair complex
MutSβ	forming heterodimeric MSH2/MSH3, component of mismatch repair complex
NER	nucleotide excision repair
NHEJ	non-homologous end joining;
NIPH	the National Institute of Public Health
NCS	neocarzinostatin, an antitumor antibiotic induces SSB and DSB, an ionizing radiation mimetic
NDZ	nocodazole, interferes with the polymerization of microtubules, G_2- or M-phase indicator
NormFinder	software using for normalization of reference gene stability
NSB1	nibrin; cell cycle regulatory protein p95; Nijmegen breakage syndrome protein 1; component of the MRE11/RAD50/NBN (MRN complex); plays a critical role in the cellular response to DNA damage and the maintenance of chromosome integrity
p21	cyclin-dependent kinase inhibitor 1; CDK-interacting protein 1
p53	tumor suppressor in many tumor types; involved in cell cycle; the p53 gene has been mapped to chromosome 17
p53pSer^{15}	p53 phospho-serine-15
p65	subunit of NF-κB; the protein is in the complex with p50 forming nuclear NF-κB
PARP	poly (ADP) ribose polymerase
PARP1	poly(ADP-ribose) polymerase 1
PBS	phosphate buffered saline; commonly used biological buffer
PCNA	proliferating cell nuclear antigen; DNA sliding clamp protein
PMS2	mismatch repair component; forms heterodimer with MLH1
Polβ	DNA polymerase β; its major role is in base excision repair as
Polδ/ε	DNA polymerase δ and ε; the main function is involvement in DNA replication

PPIA	Cyclophilin A; regulates protein folding and trafficking
qPCR	Real-Time quantitative Polymerase Chain Reaction
Rad50	DNA repair protein; component of the MRN complex, which plays a role in double-strand break (DSB) repair, DNA recombination
RFC	replication factor C; DNA-dependent ATPase; subunit of DNA polymerases; protein is important for DNA replication and repair
RNA	ribonucleic acid
ROS	reactive oxygen species; variety of molecules containing oxygen
RPA	replication protein A; required for DNA recombination, repair and replication
RT-PCR	Reverse Transcription Polymerase Chain Reaction
RT-qPCR	Real Time quantitative Reverse Transcription Polynucleotide Chain Reaction
S	cell cycle synthetic phase
SDS-PAGE	Sodium Dodecyl Sulfate Polyacrylamide Gel Electrophoresis
p53pSer^{15}	p53 phospho-serine-15
SRP	short-patch repair; sub-pathway of base excision repair
SSB	single-strand break
ssDNA	single stranded DNA
T_a	melting temperature
TC-NER	transcription-coupled nucleotide excision repair
TIFF	Tagged Image File Format; a lossless raster file format for digital images; standard graphics format for high colour depth and b/w graphics
TOP1	DNA topoisomerase I; important for the topologic states of DNA
TopBP1	DNA topoisomerase 2-binding protein 1; required for DNA replication; plays a role in the rescue of stalled replication forks and checkpoint control
Tris	tris(hydroxymethyl)aminomethane; 2-Amino-2-hydroxymethyl-propane-1,3-diol; a component of buffer solutions
Triton-X-100	polyethylene glycol p-(1,1,3,3-tetramethylbutyl)-phenyl ether; a nonionic surfactant-detergent
Tween20	polyoxyethylene (20) sorbitan monolaurate; a common detergent used in biology, in cell lysis and membrane protein solubilisation
U	uracil
UBC	ubiquitin C; is associated with protein degradation, DNA repair, reference gene
UvrD	DNA-dependent ATPase I and helicase II; facilitate DNA repair

WB	western blot; used for identification proteins with specific antibodies that were separated by gel electrophoresis
XLF/Cernunnos	non-homologous end-joining factor 1; major factor for NHEJ
XRCC4	gene functions together with DNA ligase IV; enquired for repair of double-strand breaks by the end-joining pathway
YWHAZ	tyrosine 3-monooxygenase/tryptophan 5-monooxygenase activation protein zeta; product of YWHAZ belongs to 14.3.3zeta protein family; reference gene
α-tubulin	alfa-tubulin, loading control usage
β-ME	β-mercatpoethanol
γH2AX	phosphorylated form of H2AX histone; marker of DNA double strand breaks

Definitions of terms were taken from following databases: NCBI (2016); http://www.genecards.org and Reference.MD (2016).

List of Figures

List of Tables

1 Introduction

During the DNA replication process, sometimes a non-complementary nucleotide incorporation occurs that results in the production of defective proteins. These errors introduced to the DNA strands by polymerases must be immediately repaired in order to maintain the fidelity of genetic information. Cells possess the repair systems in place, consisting of a group of proteins that proceed along the replication fork and restore the error. One of these mechanisms enables to correct the errors in replication is mismatch DNA repair (MMR) pathway. The MMR products form complexes/heterodimers of nuclear enzymes that participate in the process of error recognition. These heterodimers localize and bind to the DNA biosynthetic errors and initiate their removal. Deficiency in MMR mechanism can lead to the presence of the mutations and the phenotype of genomic instability. The end result of defects in MMR is that cell can overcome the proofreading or be silenced; which lead to cell apoptosis or unregulated proliferation resulting in tumor development.

In humans, there have been discovered nine genes involved in the MMR, five of which may be of a clinical importance. The loss of proper function one of these genes is correlated with increased susceptibility to the lifetime risk of developing cancer. For example, the mutations in *MLH1* and *MSH2* genes are studied mainly in relation to the colorectal carcinoma, where the carriers of the mutations have 70% increase in the risk of developing tumors when compared to the wild type. Recent studies point out to the importance of *MLH1* and *MSH2* genes in various tumors such as ovary, endometrium, stomach, urinary tract, as well as brain tumors. Ovarian carcinoma belongs to malignancies with the highest mortality rates among women, mostly because of the lack of early warning symptoms.

In the present diploma thesis, the unravelling of the molecular basis of repair mechanisms in the epithelial ovarian tumors was aimed at better understanding of the processes behind the DNA repair and cancer development. The primary objective of this study was to identify the candidate genes within

MMR pathway related to ovarian cancer patients. Secondary objectives were to identify the molecular mechanisms of down- or/and up-regulated candidate genes, taking to the account their regulation through the promoter silencing.

2 Aims of the thesis

- Estimation of mRNA expression profile of MMR genes
- Analysis of *MLH1* promoter methylation
- Detection of protein levels of MMR proteins
- Estimation of the role of *MLH1* in ovarian cancer cell lines

3 Literature review

3.1 DNA damage

Thousands and thousands DNA damage events occur in our cells on a daily basis and, these events can trigger to serious issues, such as malignant transformations. Many different mechanisms safeguard the DNA integrity and maintain the cell homeostasis. Living cells are well equipped to cope with the occurrence of potentially harmful events, such as DNA damage. When damage occurs, the cell faces decision between direction of life or death by activating highly conserved DNA damage pathway or cell death pathway. To improve its chances of survival, the cell has an exclusive system to halt the division until the repair is completed. This response can be described as a collective cooperation among many key players and protein partnership activations to detect and eliminate the DNA damage. The events included in this response involve the delay cell cycle progression, deal with DNA repair and engineer DNA replication (Mladenov *et al.*, 2016).

Currently, several damaging agents that constantly attack the DNA molecule causing threatening errors/breaks such as, DNA lesions, bulky adducts, intra-inter strand crosslinks or single and double strand breaks are well known. Some of these agents come from the environmental exposure (exogenous source such as irradiation, UV light, alkylating agents, and tobacco smoke), but some of them occur naturally during the cell cycle (endogenous source such as reactive oxygen species (ROS), hydrogen peroxide, products of lipid peroxidation (Sharma *et al.*, 2016; Kurfurstova D *et al.*, 2016). Each of these agents' poses recognizable mutagenic potential by attacking the DNA, resulting in incorrect base insertion, substitution, deletion or structural changes. Once DNA damage occurs, cells have to preserve the stability of genome by employing the repairing mechanisms (Helleday *et al.*, 2014).

The type of repair mechanism depends closely on the type of the arising damage. In case that only one base pair is damaged it can be processed by base excision repair (BER). BER is employed upon changes caused by deamination, alkylation, depurination/depyrimidination and oxidative damage. Sometimes

two adjacent nucleotides are damaged by sticking together. In this case, the cell employs more complex repair mechanism available, called nucleotide excision repair (NER), this mechanism consists of a set of proteins removing a short stretch of nucleotides (up to 24 nucleotides) and replacing them with the new ones while using non-damaged DNA strand as a template. NER is involved in the replication errors that interfere with the proper DNA helix conformation, such as bulky adducts, intra-inter strand crosslinks and UV photoproducts (Minocherhomji *et al.*, 2015; Bélanger *et al.*, 2016). Mismatch repair mechanism belongs to the excision repair pathways that replace inaccurate nucleotide pairing arising during DNA replication. The MMR pathway is initiated by the recognising of the incorrectly incorporated nucleotide in DNA, followed by its displacement and finalized by re-synthesis and ligation of DNA (Houlleberghs et al., 2016; Hassen et al., 2016).

Different type of DNA damage stimuli, such as X-Ray or anti-tumor agents, can lead to breaks in one or both DNA strands. Double strand breaks, biologically the most dangerous, are repaired by two most common mechanisms: non-homologous end joining (NHEJ) and homologous recombination (HR) (Vriend *et al.*, 2016; Iliakis *et. al.*, 2015; Jeggo and Löbrich, 2015.).Non-homologous end joining utilizes an undamaged DNA strand as a template, followed by the coverage of damaged strand by proteins and the replacement of damaged strand sequence by the undamaged one. Finally, the missing gaps are then completed according to complementary rule and repaired DNA results with two segments. HR repair is homology-directed repair of broken chromosomes arms, where the formation of DNA heteroduplex and annealing reactions are required. Multiple protein complexes are responsible for the resection of DNA ends, homologous DNA pairing, and synthesis-dependent strand annealing.

One of the consequences of DNA damage is the introduction of mutation into newly formed DNA strand. Some of the DNA errors are of a transient nature with the high probability to be repaired; others are creating structural alterations in the DNA. The most extreme outcome and ultimate of DNA damage is the tumor formation or establishment of disease, such as Xeroderma

pigmentosum, Ataxia-telangiectasia, Bloom's and Werner's syndromes (Ambrose and Gatti, 2013; Bischof *et al.* 2001; Lozada *et al*, 2014).

3.1.1 DNA single strand break

DNA single-strand break (SSB) is the most common damage to the DNA, occurring tens of thousands times per cell per day. SSBs are physical discontinuities in one of the DNA strands and it is usually a single nucleotide loss and 5'- and/or 3'-termini damage at the site of the break (Caldecott, 2008).

The source of the endogenous cellular SSBs is mainly due to intracellular metabolites directly attacking the DNA such as reactive oxygen species (ROS) or free radicals from hydrogen peroxide. Another source of the damage can arise from the abortive activity of the replication enzymes complex, like DNA topoisomerase 1 (TOP1). Caldecott described the role of DNA topoisomerase 1 as "TOP1 creates a 'cleavage complex' intermediate containing a DNA nick in order to relax DNA during transcription and DNA replication. These intermediates are normally transient and are rapidly resealed by TOP1. However, collision with RNA or DNA polymerases, or close proximity to other types of DNA lesion, can convert cleavage complexes into TOP1-linked SSBs (TOP1–SSBs) or TOP1-linked DSBs (TOP1–DSBs), in which TOP1 is covalently linked to the 3'-terminus of the DNA strand break" (Caldecott, 2008; Wang, 2002; Pommier, 2003).

3.1.2 DNA double strand break

DNA double-strand break activates two main pathways: Non-homologous end joining (NHEJ) divided into i) classical-non-homologous end-joining, c-NHEJ; ii) alternative NHEJ (or simply alternative EJ) and Homologous recombination (HR).

Classical non-homologous end joining is an error-prone pathway. The broken DNA duplex is processed by the complex of enzymes, where each site of the break is recognised and processed by Ku70/80 and DNA-dependent protein kinase catalytic subunit (DNAPKcs) (Rivera-Calzada *et al.*, 2007). The initial recognition of DSBs is established through the binding of Ku70/80 heterodimer

to the broken ends. Ku70/80 then leaves the broken ends exposed and recruits DNAPKcs, resulting in the recruit of the nuclease Artemis and is capable of phosphorylating H2AX on serine 139 within the nucleosomes. Phosphorylated H2AX is acting as a DSB marker with the role in DDR pathway and chromatin remodelling (Turinetto and Giachino, 2015). Artemis trims single nucleotides at the break site and ligase IV/XRCC4 ligates the broken ends together, result in the re-connection of the duplex (Lieber, 2010). This reaction is enhanced by XLF/Cernunnos, which interacts with XRCC4 (Iliakis *et al.*, 2015) (Figure 3.1). In alternative joining, the processing of DSBs is arranged by PARP1 and MRE11-Rad50-NBS1 complex (simply called MRN complex) and free DNA ends are repaired to rescue DNA replication forks (Costantino *et al.*, 2014; Iliakis *et al.*, 2015). MRN complex is the main protein involved in the multiple processes including the homologous recombination repair as well as in the DNA damage response.

Homologous recombination occurs in the process of meiosis but it can also repair double strand breaks during S and G_2 stages of the cell cycle. HR is highly evolutionary conserved, error-free repair mechanism. DSB creates 3'-single overhangs on DNA, through a process called resection. Resection is mediated by MRN complex with dual endo- and exonuclease activities; the endonuclease activity is stimulated by CtIP protein. The formation of 3′-tailed overhangs is coated by RPA protein and serves as a substrate for the recombinase protein Rad50 coiled-coils. Recent hypothesis on the importance of Rad50 coiled-coils in HR is to tether the two DNA ends together (Lafrance-Vanasse *et al.*, 2015) (Figure 3.1).

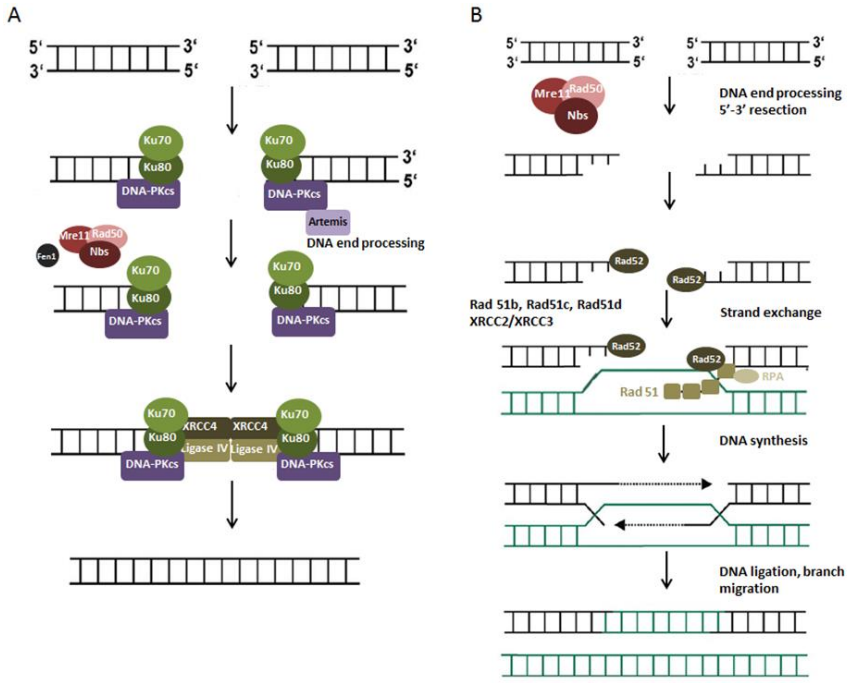

Figure 3.1. Schematic model of main pathways of DSB A) non-homologous end joining, it's summary of resection, initial steps through binding KU70/80/DNAPKcs complex, Artemis DNA processing and final step of DNA end ligation **B)** homologous recombination, recruitment of MRN complex following DNA resection. After resection, HR continues by formation of DNA heteroduplex that resulting in strand exchange followed by it ligation. (Figure is adapted from Leyns and Gonzalez, 2012)

3.1.3 DNA damage response

In Eukaryotes, the cellular response to DNA damage is orchestrated by DNA damage response pathway. This cell response to DNA damage danger and its ability to repair damage stimulates the cell cycle checkpoint activation that results in the cell cycle arrest.

Single stranded DNA is rapidly coated by RPA protein. DNA coated by RPA can recruit ATRIP (ATR interacting protein)/ATR (ATM and Rad3-Related) and promotes ATR trans-autophosporylation (Marenchal and Zou, 2013). RPA also recruits Rad17 (Rad17-replication factor C) clamp loader and 9-1-1 proteins have the affinity to the protein TOPBP1 - direct activator of ATR. Activated ATR phosphorylates Chk1 kinase substrate, resulting in the activation of downstream effectors such as the cell division cycle 25 (CDC25) phosphatase, that is further involved in many cellular processes (Sulli *et al.*, 2012).

On the other hand, DSB is sensed by MRN complex and activated through the phosphorylation of ATM (Ataxia-telangiectasia mutated) that subsequently phosphorylates the downstream kinases Chk2, p53, BRCA1 and H2AX (phosphorylated form is known as γH2AX). The initial activation of ATM by DSB triggers the accumulation of γH2AX within the minutes the damage event (Marenchal and Zou, 2013). Phosphorylated variant of H2AX is recognized by an important mediator Mdc1 that directly to binds γH2AX. Mdc1 has an ability to interact with both γH2AX and ATM, and enables ATM to target nucleosome. Afterwards, the p53 protein can be phosphorylated at Ser^{15} directly by ATM or indirectly via Chk2; and this phosphorylation leads to the activation of p21 transcription, that is Cdk inhibitor (Sengupta and Harris, 2005; Leyns and Gonzalez, 2012). Encoded p21 binds and inhibits Cdk2/4 complexes, functioning as a regulator of G1 cell cycle progression. Similar to Chk1, the active Chk2 also leads to the degradation of CDC25 phosphatase a key player needed for Cdk2 phosphorylation that is further required for G1/S phase transition.

Importantly, the ATR and ATM specific inhibitors become available for the cancer treatment, already with the promising clinical outcomes (Benada and Macurek, 2015, Kwok *et al.*, 2016; Albarakati N *et al*, 2015; Vendett *et al.*2015; Knittel G *et al.*, 2015; Abu-Sanad *et al.*, 2015).

3.2 DNA damage repair

DNA repair is the collective process by which cell can identify and correct of the DNA damage introduced by the endo- and/or exogenous insults. Each step during the repair processes requires the verification in order to increase its specificity. DNA repair safeguards the genome stability resulting in the protection of many essential biological processes.

3.2.1 Base excision repair

Base excision repair (BER) to repairs DNA errors induced via the miscoding base lesions from the oxidation, deamination, and alkylation processes. During the initial step, DNA glycosylase recognises and excises a single damaged base

followed by the removal of damaged nucleotide by AP endonucleases and the insertion of the correct base that is executed by DNA polymerase ß. The final step is concluded by the utilisation of DNA ligase, which seals the DNA strand.

The BER has two sub-pathways, short-patch repair (SPR) and long-patch repair (LPR), while in SPR is single nucleotide correction, repair machinery is based on the cooperation of Pol ß and ligation of the DNA strands via XRCC1 and Ligase III. Meanwhile, LPR is utilised for the repair of multiple nucleotides via PCNA, Pol δ/ε and FEN 1 complex, where the transient DNA ends are again sealed together by Ligase I (Rahmanian *et al.*, 2014) (Figure 3.2).

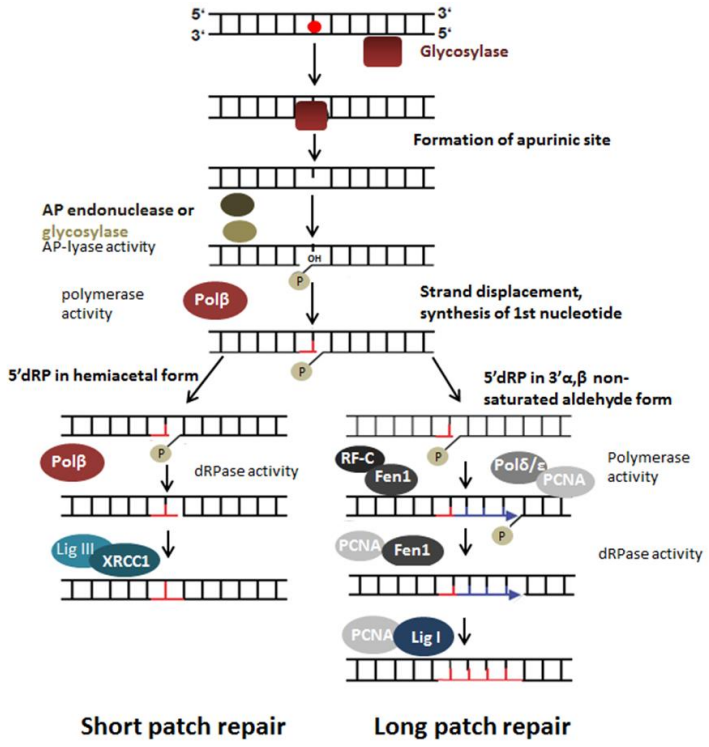

Figure 3.2. Model of Base excision repair. The initial recognition in BER is done by DNA glycosylase; followed by base removal; and the choice between short and long patch depends on the 5'terminus. Final step is sealing of the DNA ends by ligase III (left) or ligase I (right) (Figure is adapted from Leyns and Gonzalez, 2012)

3.2.2 Nucleotide excision repair

Nucleotide excision repair (NER) is a key cellular process employed in the response to the DNA damage that protects the genomic integrity against endogenous and exogenous insults such as mutagenic chemicals, UV radiation, or chemotherapeutic drugs.

NER has two cellular pathways: i) transcription-coupled NER (TC-NER) – which removes lesions from the transcribed strand of active genes and ii) global genome nucleotide excision repair (GG-NER) which removes the lesion from non-transcribed strand. Formation of DNA adducts results in the recruitment of NER machinery for its removal, ssDNA is covered by the RPA protein and specific endonucleases are used to cut and remove the bulky structures. The occurrence of the momentarily opened DNA strand calls for the repair synthesis, followed by the gap sealing with DNA ligase; resulting in the chromosome restoration (Sertic, 2012) (Figure 3.3).

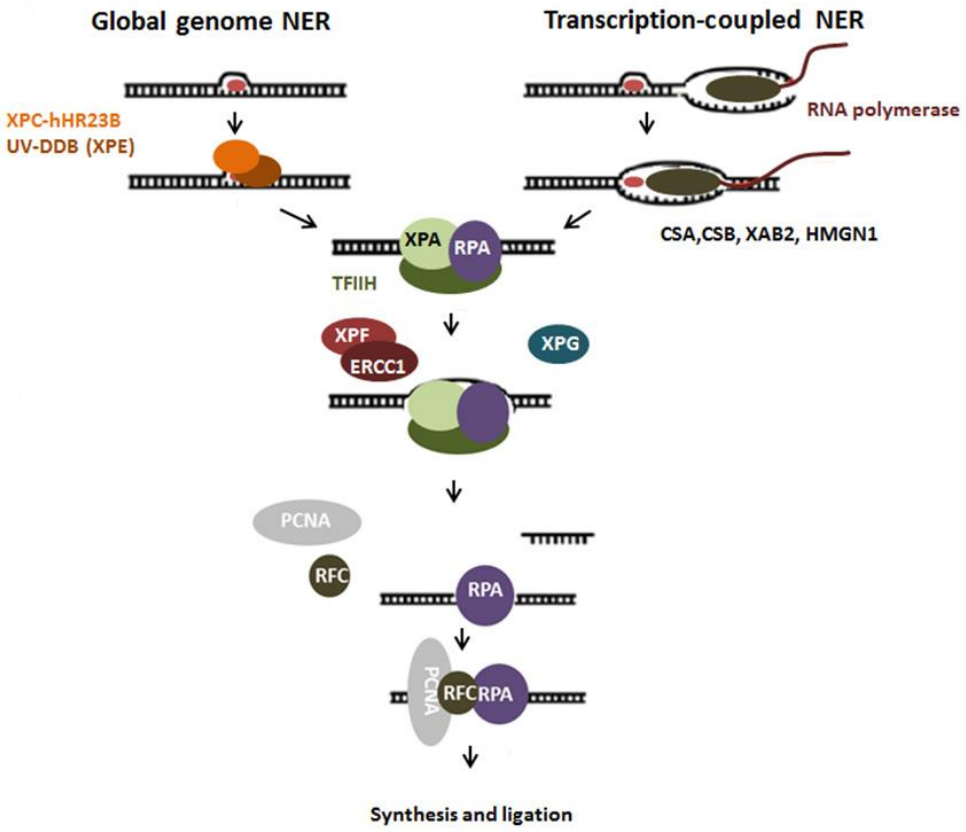

Figure 3.3. Model of Nucleotide excision repair. Two main NER pathways including XPC-HR23B and UV-DDB recognize damaged nucleotide and initiate GG-NER. TC-NER RNA polII is blocked and followed by merged pathway orchestrated by RPA, TFIIA and XPA complex unwinding the DNA strand. Next step includes excision of damaged nucleotide by XPF/ERCC1. Final step covers DNA synthesis and ligation by ligases. (Figure is adapted from Leyns and Gonzalez, 2012)

3.2.3 Mismatch repair pathway

Mismatch repair (MMR) is a cellular response to DNA mispaired errors arising during the DNA replication and genetic recombination. It is a highly conserved editing system that corrects misincorporation of nucleotide, controls the mutation rates in response to various types of DNA damage including environmental changes or chemotherapy treatment. During the DNA replication, DNA polymerases integrate erroneous bases with the frequency of 1:10,000 to 1: 100,000 (Jiricny, 2013; Arana and Kunkel, 2010). Moreover, all replicative polymerases are efficient in providing of the exonuclease proofreading and have the ability to remove nucleotides from the 3'end of the daughter strand. Those miss-paired nucleotides that have escaped the DNA polymerase proofreading are then recognised by the MMR proteins (Jiricny, 2013).

The machinery of MMR includes core enzymes, in humans, the mis-paired bases are recognised by the heterodimers MutSα (MSH2/MSH6), MutSβ (MSH2/MSH6). The canonical MMR cascade is replication based, and covers four steps i) mismatches detection by heterodimeric MutSα (MSH2/MSH6), MutSβ (MSH2/MSH6) (Groothuizen and Sixma, 2016). ii) Mismatch detection triggers ATP-dependent sliding clamp proteins which result in mismatch release and diffusion along the DNA helix (Hingorani, 2016). iii) MLH1/PMS2 complex formation with endonuclease activity. iv) the incorrect nucleotide replacement (Tham, 2015) (Figure 3.4).

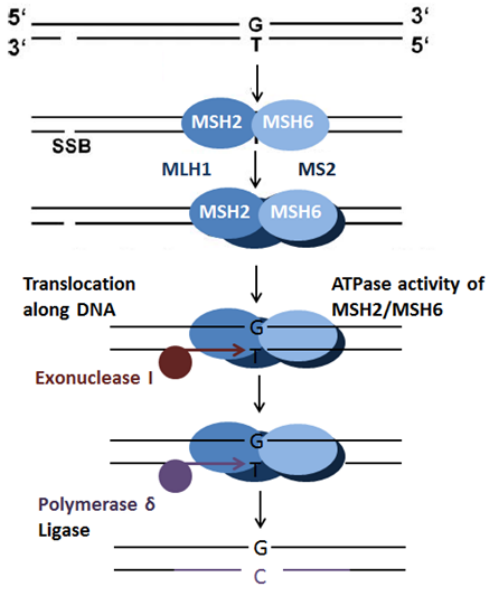

Figure 3.4. Model of Mismatch repair. The mismatch recognition by heterodimer MSH2/MSH6, and together with MLH1 initiates the repair. Exonuclease-mediated degradation of mis-base by EXO1 and the correct nucleotide insertion by DNA polymerase δ (figure is adapted from Leyns and Gonzalez, 2012)

The key proteins of MMR are evolutionarily conserved and consist of the heterodimeric sensors and ATPases. A well-established model for understating of the MMR pathway mechanism is known from the bacteria Escherichia coli and involves five repair processes.

First, the MutS protein recognizes and binds to the base-base mismatch DNA sequence. Second, the MutS binds to ATP and forms ATP-induced sliding clamp. Third, the MutS undergoes the conformation changes and as a sliding clamp binds to MutL, which promotes the endonuclease and helicase activity. Four, the MutS is released from DNA and hydrolyses ATP. Endonuclease activity is regulated by endonuclease MutH (humans homologs PMS2 or MLH3), which is capable of recognising newly synthesised strand by the absence of adenine methylation (GATC) at daughter strand. MutH is able to make a nick in the daughter strand and the helicase UvrD activated by MutL, unwinds the DNA from the nick. Five, the DNA is resynthesized by the DNA polymerase III, following DNA ligation by ligase (Groothuizen, 2016).

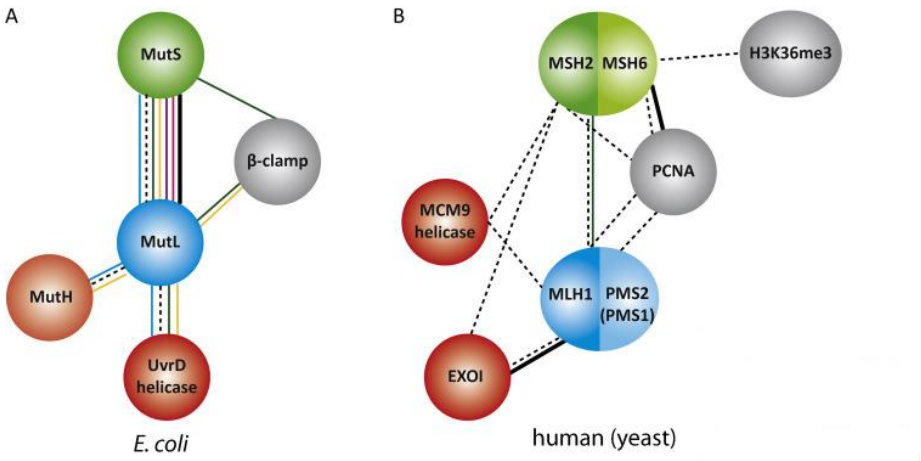

Figure 3.5. Schematic model of MMR protein interactions A) E.coli **B)** Human grey proteins represent replication machinery and red colored MMR effector proteins (figure is adapted from Friedhoff, 2016)

In Eukaryotes, the mis-paired errors are recognised by the five di/heteromeric proteins, namely MutSα (composed of MSH2/MSH6 in humans), MutSß (MSH2/MSH3), MutLα (MLH1/PMS2), MutLß (MLH1/PMS1) and MutLγ (MLH1/MLH3). In humans, a heterodimer MSH2/MSH6 recognizes a mis-paired base, in the same manner as MSH2/MSH3 recognizes the longer

insertions and deletions. MLH1/PMS2 is a part of the MutLα complex and MLH1/MLH3 has a redundant function (Groothuizen, 2016) (Figure 3.5, Table 3.6). The interaction between MutSα and MutLα has been studied and a new enzyme, the helicase MCM9, was discovered to play an important role in human MMR system. Furthermore, interaction of MMR machinery with replication machinery has been demonstrated (Traver *et al.*, 2015).

In recent studies, MutSα and MutLα have been confirmed to interact with the replicative DNA polymerases, PCNA and the MutSα forms a clamp protein that slides alongside the DNA strand. This process requires the use of ATP on MutSα. The homodimeric clamp protein and PCNA are loaded into free 3'end of DNA strand by polymerase III and/or replication factor C (RFC). These complexes then help to establish the DNA-protein-substrate interactions, through the highly conserved motifs. Initially, in S-phase PCNA recruits MMR enzymes to the replication fork, PCNA in endowed high affinity to MSH3 and MSH6, which is required to down-stream processes and is involved in activation of MutLα endonuclease. Following experiments lead to the discovery of a new player in the MMR pathway, exonuclease 1 (EXO1) with the 5'-3'exonuclease activity. MutLα endonuclease activity generates the additional breaks in the 3'-nicked strand between the nick and ~ 150 nucleotides downstream the mismatch site. These additional breaks form a loading site for EXO1 that is able to erase the DNA in a 5'-3' direction and the resulting single strand gap is filed in with the polymerase δ and ligase I (Jiricny, 2012).

Additionally, the phosphorylation of tyrosine 211 on PCNA by the epidermal growth factor receptor (EGFR) inhibits the MMR by introducing the inadequate interaction between phosphorylated PCNA and MutSα. Activation of MutSα depends on PCNA and this binding ensures proper MMR down-stream response (Friedhoff, 2016).

Table 3.6. Overviews of human mismatch repair proteins

Protein	Heterodimer	Function	Reference
MutS	MSH2/MSH6 MSH2/MSH3	Mismatch recognition; ATP-binding sliding clamp protein formation	Jeon et al., 2016
MutL	MLH1/PMS2 MLH1/PMS1 MLH1/MLH3	MMR downstream processes activator	Kadyrova and Kadyrov, 2016
PCNA	PCNA	Binds MMR machinery to replication fork	Kanu *et. al*, 2015
EXO1	EXO1	5' – 3' excision	Myler *et. al.*, 2016
MCM9	MCM9	Helicase activity	Jeffries *et. al.*, 2013
RFC	RFC complex	ß- clamp loading	Sakato *et. al.*, 2012

3.2.4 Cancer associated mismatch repair

Correctly functional mismatch repair reduces the mutation rate and prevents the cancer development through the maintenance of the genome stability or the induction of the cell death. The mutations in the MMR genes decrease the genome stability and are etiological factors for the occurrence of certain cancers. The germline mutation of MMR genes is involved in the Lynch syndrome, known also as the hereditary non-polyposis colorectal cancer (HNPCC). The majority of the mutations are found in *MLH1* (42%), *MSH2* (33%), *MSH6* (18%), or *PMS2* (7.5%) genes and are leading to these genes dysfunction (Begum and Martin, 2016). Furthermore, frameshift mutations resulting in truncated form of the proteins, inhibit the MMR protein function. Moreover, the nonsense and missense mutations affecting a single amino acid in MMR proteins are frequently seen in the pathophysiological cancer conditions. Patients usually have a mutation in one allele and upon somatic loss of the wild-type allele, MMR-homozygote mutated cells undergo malignant transformation. Gene silencing is not always due to the loss of heterozygosity, but due to an epigenetic alterations such as the promoter methylation. Transcriptional inactivation via the promoter hypermethylation of *MLH1* gene causes microsatellite instability (MSI), which is commonly diagnosed in the colorectal tumors (Haraldsdottir *et al.*, 2016; Kidambi *et al.*, 2016; Sahnane et al., 2015).

Microsatellites, short tandem repeats, are widely spread across the DNA, loss of MMR gene function lead to replication errors, resulting in the higher rate of the microsatellite instability often found in the tumors. Microsatellite instability is a result of hypermutable phenotype and the standard panel of at least of 5 microsatellites is analysed by PCR, where the introduction of the instability is detected by either loss or gain in microsatellite length. In case that more than two microsatellites are mutated, the tumor is classified as a microsatellite-high (MSI-H), if only one microsatellite in mutated - the tumor is microsatellite-low (MSI-L). Tumors with the mutation in *MLH1* or *MSH2* are usually categorized as MSI-H, whereas the mutations in *MSH6* or *PMS2* are referred as MSI-L (McConechy *et al.*, 2015; Duraturo *et al.*, 2015).

Moreover, another epigenetic event, i.e. regulation by non-coding RNAs seems to be important in the process of developing a carcinoma. Recent studies elucidated that miRNAs are regulating thousands of genes by facilitation of the mRNA degradation. mRNA of *MLH1*, *MHS2*, and *MSH6* genes are targeted and deregulated by miRNAs, specifically by miRNA-21 and miRNA-155 (Begun and Martin, 2016). Interestingly, microsatellite instable tumors and microsatellite stable tumors appear to be targeted by different miRNAs, thus this knowledge can be essential for the clinical diagnosis (Peña-Diez and Rasmussen, 2016).

Above all, recent studies claim that the defects in the MMR pathway increase the risk of developing endometrium, ovaries, and stomach cancers (Hemminki et al., 2003).

3.3 Epigenetic mechanisms

3.3.1 Promoter methylation

Currently, one of the most important and most studied epigenetic mechanism is DNA methylation. DNA methylation is a covalent attachment of a methyl group (-CH3) that occurs on the cytosine residues to form 5-methylcytosine (5mC) (Schofield and Hsieh, 2003). Specific small DNA regions enriched with the GC dinucleotides, known as CpG islands, are usually methylated by the DNA methylases. These islands are often clustered nearby the regulatory regions

such as gene promoters. While the CpG islands in the promoter regions remain unmethylated in the healthy tissues, silencing the promoter CpG islands by methylation affects the transcriptional regulation and might play a role in the tumor development (McCabe *et al.*, 2009; Curradi *et al.,* 2002).

Importantly, many changes in DNA methylation patterns in tumors are associated with the use of the chemotherapeutic treatments. The chemoresistance to chemotherapeutics such as cisplatin commonly used in the treatment of ovarian cancers is the critical response to DNA methylation (Zeller *et al.*, 2012). Multiple DNA epigenetic changes including promoter region methylation were observed in cisplatin-resistant cancer cells with the gene silencing effect. For example, the gene with the chemoresistance response is MLH1 mismatch repair, is observed in about 25–35% of ovarian cancer patients. DNA repair deficiency due to the promoter methylation silencing leads to the chemotherapy resistance, gene mutation and poor survival prognosis (Zeller *et al.*, 2012; Shilpa *et al.*, 2014; Farkas *et al.*, 2014; Gao *et al.*, 2016).

3.4 Molecular pathology of Ovarian cancer

Approximately, 90% of all ovarian cancers are characterized as epithelial ovarian cancer (EOC) and up to 75-80% are diagnosed in the late the stages of the disease development. According to the histopathological criteria's four different subtypes are distinguished comprising serous, mucinous, clear cell, and endometrioid carcinoma (Prat, 2014).

The majority of EOC tumors are classified as Grade I - III, where Grade I is characterised as tumors with low chromosomal instability and with a high frequency of mutations in *KRAS* and *BRAF* genes. The Grade II tumors have high frequency of p53 mutations and high chromosomal instability. The Grade III is characterized as a metastatic with tendency to grow and spread quickly.

Up to 10 % of EOC tumors are diagnosed as those bearing *BRCA1* and *BRCA2* mutations. Both *BRCA1* and *BRCA2* are important proteins involved in the repair pathways and are critical for the repair of DSBs by HR (Prakash *et al.*, 2015). A loss of their functions result in increased cancer risk in general.

Furthermore, BRCA dependent cancers, including ovarian cancers, are potentially predisposed to targeted treatment through induced cell death.

According to FIGO (The International Federation of Gynecologists and Obstetricians), the standard classification used for ovarian cancer staging is shown below.

Stage I: - Tumor confined to ovaries or fallopian tube(s)

Stage II: - Tumor involves one or both ovaries or fallopian tubes with pelvic extension (below pelvic brim) or primary peritoneal cancer

Stage III: - Tumor involves one or both ovaries or fallopian tubes, or primary peritoneal cancer, with cytologically or histologically confirmed spread to the peritoneum outside the pelvis and/or metastasis to the retroperitoneal lymph nodes (Prat, 2014)

Stage IV: - Distant metastasis excluding peritoneal metastases

Knowing the molecular pathogenesis of EOC and the signalling background is the promising approach for increasing and identifying the effective treatment. The high mortality is due to advanced stages of ovarian cancer. The absence of effective screening, biomarkers, and late diagnosis, lead to the high mortality caused by EOC. The 5 years survival time after diagnosis is caused by the lack of specific symptoms in early stages, late diagnosis and chemoresistance towards drugs. Identifying non-invasive biomarkers specific for early stages is crucial for the increase in the survival rate.

The most well-studied and clinically used biomarker of EOC is a glycoprotein Carbohydrate antigen (CA-125). Well-established CA-125 is overexpressed in EOC and can be identified in patients bloodstream, despite the detection in EOC the CA-125 is elevated in many benign states as well as in endometriosis and uterine fibroids (Gloss, 2012). The specificity of CA-125 is 97% is in advanced epithelial cancer (type III and IV), but it's decreased in grade I. Therefore, CA-125 alone is unacceptably unsuited as a diagnostic marker and improved additional screening with higher specify, is necessary (Sölétormos *et al.*, 2016; Bottoni and Scatena, 2015; Dikmen *et al.*, 2015). In addition, novel

non-invasive biomarkers, specific for each subtype of EOC are required to increase early detection.

4 Material & methods

4.1 Material

4.1.1 Chemicals and material

Table 4.1. List of chemicals and material

Chemical	Source
10 mM dNTPs (deoxynucleotide triphosphates)	Fermentas International Inc., Burligton, USA
Acrylamid/Bis 30%	Serva Electrophoresis GmbH, Heidelberg, Germany
Agarose	Serva Electrophoresis GmbH, Heidelberg, Germany
Ambion® Nuclease-Free Water	Thermo Fisher Scientific Inc, Waltham, MA USA
Amersham Hyperfilm ECL	GE Healthcare; BioTech a.s., Prague, Czech Republic
APS (ammonium persulfate)	Sigma Aldrich, St. Louis, USA
BCA assay kit (Bicinchoninic acid kit)	Pierce, Rockford, IL, USA
Chloroform	Sigma Aldrich, St. Louis, USA
Designed Primers	Sigma Aldrich, St. Louis, USA
DNasy Blood® & Tissue Kit	Qiagen, Hilden, Germany
DNeasy® Blood & Tissue Kit	Qiagen, Venlo, Netherlands
Dulbecco's modified Eagle's medium	Sigma Aldrich, St. Louis, USA
EpiTect® Bisulfite Kit	Qiagen, Hilden, Germany
Ethanol 96%	Penta, Prague, CR
Ethidium bromide	Sigma Aldrich, St. Louis, USA
Fetal bovine serum	Sigma Aldrich, St. Louis, USA
GeneRuler™ 1 kb DNA Ladder	Fermentas International Inc., Burligton, USA
High-Capacity cDNA Reverse Transcription Kit	Thermo Fisher Scientific Inc, Waltham, MA USA
Loading Dye Solution 6x	Fermentas International Inc., Burligton, USA
MagNA Lyser Instrument	Roche Diagnostics GmbH, Mannheim, Germany
MagNA Lyser Green Beads	Roche Diagnostics GmbH, Mannheim, Germany

Continued on next page

Table 4.2. Continued from previous page

Chemical	Source
Methanol	Penta, Prague, CR
NaCl (Sodium chloride) 99%	Pliva – Lachema a.s., Brno, Czech Republic
Nonfat dry milk	Migros, Zurich, Switzerland
PageRuler prestained protein ladder	Fermentas International Inc., Burligton, USA
PBS (Phosphate buffered saline)	Media preparation unit, IMG ASCR, v.v.i., Prague, CR
Penicillin	Thermo Fisher Scientific Inc, Waltham, MA USA
Ponceau S	Bio-Rad Laboratories, Hercules, USA
Protease inhibitor cocktail tablets	Roche Diagnostics GmbH, Mannheim, Germany
RNase inhibitor	Thermo Fisher Scientific Inc, Waltham, MA USA
RNeasy Plus Mini Kit	Qiagen, Hilden, Germany
RNAlater® Solutions	Thermo Fisher Scientific Inc, Waltham, MA USA
SDS (sodium dodecyl sulfate)	Serva Electrophoresis GmbH, Heidelberg, Germany
Streptomycin	Thermo Fisher Scientific Inc, Waltham, MA USA
TaqMan® Expression Assay	Thermo Fisher Scientific Inc, Waltham, MA USA
TaqMan® MicroRNA Reverse Trancription Kit	Thermo Fisher Scientific Inc, Waltham, MA USA
TaqMan® Universal PCR Master Mix	Thermo Fisher Scientific Inc, Waltham, MA USA
Tri Reagent	Sigma Aldrich, St. Louis, USA
Tris (Tris(hydroxymethyl)aminomethane)	Fluka, St. Gallen, Switzerland
Triton X-100	Fluka, St. Gallen, Switzerland
Whatman Protran® nitrocellulose membrane	Whatman plc, Maidstone, Kent, United Kingdom

Table 4.3. List of used primary antibodies

Antibody	Host	Source	Cat.No.	WB
MLH1	m/mono	Cell Signaling, Technology Inc., Denvers, USA	#3515	1000×
MSH2	rb/mono	Cell Signaling, Technology Inc., Denvers, USA	#2017	1000×
PMS1	rb/poly	Cell Signaling, Technology Inc., Denvers, USA	#3996	1000×
α-tubulin	m/mono	Santa Cruz Biotechnology Inc, Santa Cruz, USA	sc-8035	1000×
anti-BrdU FITC		BD Biosciences, San Jose, USA	# 347583	500×
pH3	rb/poly	Merck Millipore, Darmstadt, Germany	#06-570	500×

Abbreviations: rb- rabbit; m - mouse; poly – polyclonal; mono – monoclonal; WD - working dilution for western blot from original stock

Table 4.4. List of used secondary antibodies

Antibody	Host	Source	Cat.No.	WB
Anti-mouse IgG, HRP-linked	Goat	Cell Signaling, Technology Inc., Denvers, USA	#7076	5000×
Anti-rabbit IgG, HRP-linked	Goat	Cell Signaling, Technology Inc., Denvers, USA	#7074	5000×
Anti-mouse Alexa Fluor® 647 conjugate	Goat	Thermo Fisher Scientific Inc, Waltham, MA USA	# A21236	500×

Abbreviations: HRP - horseradish peroxidase; IgG – immunoglobin WD - working dilution for western blot from original stock

4.1.2 List of used instruments and other equipment

Table 4.5. List of used instruments and other equipment

Instrument	Manufacturer
ABI Prism 7300 Real-Time PCR System	Applied Biosystems, Foster City, USA
BioSafety Cabinet (laminar hood) Bio-II-A	Telstar, Barcelona, Spain
Centrifuge 5424 Eppendorf	Eppendorf,Hamburg, Germany
Gilson PIPETMANs Neo® Set	Gilson, Inc., Middleton, USA
Hettich® MIKRO 120 centrifuge	Sigma Aldrich, St. Louis, USA
HRM cycler	Eco Illumina, San Diego, USA
Laminar Flow Biosafety Cabinets	Bristol, USA

LightCycler 480	Roche Diagnostics GmbH, Mannheim, Germany
Methyl Primer Express Software 1.0	Applied Biosystems, Foster City, USA
MJ Research PTC-200 PCR thermocycler	GMI, Ramsey, USA
Multi-Spin MSC-3000	Biosan, Riga, Latvia
NanoDrop® ND-1000 Spectrophotometer	Thermo Fisher Scientific Inc., Waltham, USA
Proline® Plus mechanical pipette	Biothit, Helsinki, Finland
UV Transilluminator	East Port, Prague, Czech Republic
Vortex Lab dancer	VWR, Darmstadt, Germany

4.1.3 Collection of biological material

In this study, the analysis was performed using the same set of samples of 63 ovarian epithelia tumors and 12 healthy ovary tissues that were collected in assistance of Radka Václavíková, Ph.D. from The National Institute of Public Health (NIPH); Prof. Lukáš Rob, M.D, Ph.D. from Motol University Hospital. Samples were obtained from patients diagnosed with ovarian carcinoma with surgical resection of tumor tissue. The control samples were collected from independently from healthy female donors. Collections of biological material have been approved by the ethical committees in the framework of the relevant projects. All tissue samples, isolated RNA and DNA were stored in at -80 ° C.

4.2 Methods

4.2.1 DNA and RNA isolation

Tissues were added and stored at RNAlater® stabilization solution at -80°C for long storage.

Approximately, 6 mm^3 of the tissue was used for DNA and/or RNA isolation. Tissue was disrupted and homogenized by MagNA Lyser Green Beads using the MagNA Lyser Instrument.

The genomic DNA (gDNA) extracted by using DNeasy® Blood & Tissue Kit according to manufacturer's protocol using QIAGEN anion-exchange technology. The principle of the method is denaturation of proteins, such as nucleases, histones, DNA binding proteins, metabolites, cytoplasmic and

membrane proteins by provided lysis buffer. Under the pH and low-salt conditions DNA binds to the column while the rest of the lysate flow through the column. Isolated DNA was washed and eluted in Ambion® Nuclease-Free Water.

Total RNA was isolated by using RNeasy® Plus Mini kit according to the manufacturer's protocol. Completely homogenized tissue was lysed by RLT Buffer containing β-mercaptoethanol (β-ME) and transferred to qDNA eliminator spin column. After centrifugation 30s at ≥ 8000× g RT, the lysate was transferred into RNeasy spin column and washed twice with washing buffer contained 96% ethanol. Next, the RNeasy spin column was placed in a new collection column centrifuged 1 min at ≥ 8000× g RT to let the membrane dry. Then, the RNase-free water added directly to the spin column; centrifuged 1 min at ≥ 8000× g RT to elute the RNA. The pellet was incubated at 58 °C for 5 minutes.

The concentration of samples was measured via NanoDrop® ND-1000 Spectrophotometer. The ratio of absorbance at 260 nm and 280 nm was used to assess the purity of DNA and RNA. A ratio of ~1.8 is generally accepted as "pure" for DNA; a ratio of ~2.0 is generally accepted as "pure" for RNA. All our samples passed these criteria's for further analysis.

4.2.2 RT-qPCR

Reverse transcription PCR (RT-PCR)

The conversion from RNA to cDNA using reverse transcriptase and dNTPs included in High-Capacity cDNA Reverse Transcription Kit. In the first step, RT master mix was prepared according to the manufacturer's protocol (Table 4.6). Total RNA in concentration of 200 ng per 20 µl was converting for each sample to cDNA. The RT PCR was performed on PTC-200 PCR thermocycler (Table 4.7) and secondly, cDNA stored at -80°C for long term storage.

Table 4.6. RT-PCR master-mix and RNA samples mixture (per one reaction)

Component	Volume/reaction (µl)
10x RT Buffer	2
25x dNTP Mix (100mM)	0.8
10x RT Random Primers	2
MultiScribe™ Reverse Transcriptase	1
RNase inhibitor	1
Nuclease-free water	3.2
RNA (100 µg/µl)	2
Total volume	**20**

Table 4.7. RT-PCR program setting

Step	Temperature (°C)	Time(min)
1	25	10
2	37	120
3	85	5
4	4	forever

Quantitative reverse transcription PCR (RT-qPCR)

Two-step quantitative reverse transcription PCR was performed on ABI Prism 7300 using TaqMan® Gene Expression Assays (Table 4.8). The PCR master mix and cDNA mixtures were prepared as described in the Table 4.9. In this step, the DNA polymerase amplifies target cDNA using sequence-specific primers and the TaqMan® probe in program settings in the Table 4.10. The relative cDNA amount was estimated by a standard curve, data normalized to, *UBC, YWHAZ* and *PPIA*.

Table 4.8. TaqMan® Gene Expression Assays. MMR genes quantification assays used for qPCR

Gene	Probe ID	Transcript
MLH1	Hs00179866_m1	7 RefSeqs (NM)
MLH3	Hs00271778_m1	2 RefSeqs (NM)
MSH2	Hs00953523_m1	1 RefSeq (NM)
MSH3	Hs00989003_m1	1 RefSeq (NM)
MSH6	Hs00264721_m1	2 RefSeqs (NM)
PMS1	Hs00922262_m1	3 RefSeqs (NM)
PMS2	Hs00241053_m1	1 RefSeq (NM)
TOP1	Hs00243257_m1	7 RefSeqs (NM)
ACTB	Hs99999903_m1	1 RefSeq (NM)
GAPDH	Hs02758991_g1	2 RefSeqs (NM)
B2M	Hs00984230_m1	1 RefSeq (NM)
YWHAZ	Hs03044281_g1	6 RefSeqs (NM)
UBC	Hs00824723_m1	1 RefSeq (NM)
HPRT1	Hs02800695_m1	1 RefSeq (NM)
GUSB	Hs00939627_m1	1 RefSeq (NM)
18S	Hs03003631_g1	-
EXO1	Hs01116195_m1	3 RefSeqs (NM)
PPIA	Hs04194521_s1	1 RefSeq (NM)

Table 4.9. PCR master-mix and RNA samples mixture (per one reaction)

Component	Volume/reaction (µl)
2x TaqMan®Universal Master Mix	10
20x TaqMan®Gene Expression Assay	1
cDNA template (50ng) + nuclease-free water	9
Total volume	**20**

Table 4.10. RT-qPCR program setting including dissociation analysis

Step	Temperature (°C)	Time(min)
1	50	2
2	95	10
3	95	0:15
4	60	1
5	*40×*	*repeated the step 3 and 4*
7	4	forever

4.2.3 Methyl-sensitive high resolution melting MS-HRM

CpG islands or CpG sites were identified by using Methyl Primer Express Software 1.0 (Applied Biosystems, Foster City, CA). The same software was used for primer design of DNA bisulfite conversion. The criteria of primer design were the number of CpG sites in the PCR amplicon, as well as the melting temperature (T_a). Verification of the correct length of the PCR products and undesirable primer-dimers, the 2% of agar gel was prepared.

Bisulfite conversion of DNA

The DNA in 30 ng/µl of concentration was used for bisulfite conversion which deaminates unmethylated cytosines (C) to form uracil (U), but does not affect methylated cytosines. The column based EpiTect Bisulfite Kit enable complete conversion of unmethylated cytosine to uracil in reactions.

According to the manual EpiTect® Bisulfite Handbook, the following steps are required, bisulfite-mediated conversion of unmethylated cytosines; binding of the converted single-stranded DNA to the membrane of an EpiTect spin column; washing; desulfonation of membrane-bound DNA; washing of the membrane-bound DNA to remove desulfonation agent; and elute the DNA in nuclease-free water. Bisulfite thermal cycling is illustrated in the Table 4.11.

Table 4.11. Bisulfite conversion program setting according to the manufacture's protocol

Step	Temperature (°C)	Time (min)
1	95	5
2	60	25
3	95	5
4	60	85
5	95	5
6	60	175
7	20	forever

MS-HRM method

The signal detection and analysis of methylation were obtained by using commercially available kits EpiTect® HRM™ PCR Kit and EpiTect® Control DNA ™ (100% methylated and unmethylated 100% control DNA) (Figure 4.12), and run by MS-HRM by using LightCycler 480. MS-HRM master-mix and converted DNA samples mixture (per one reaction) are illustrated in (Table 4.13) The 2% of agarose gel was prepared and gels were run in the TAE buffer (Tris-acetate-EDTA; pH 8.0) at constant voltage 100 V. DNA was visualized by ethidium bromide and UVtransluminator.

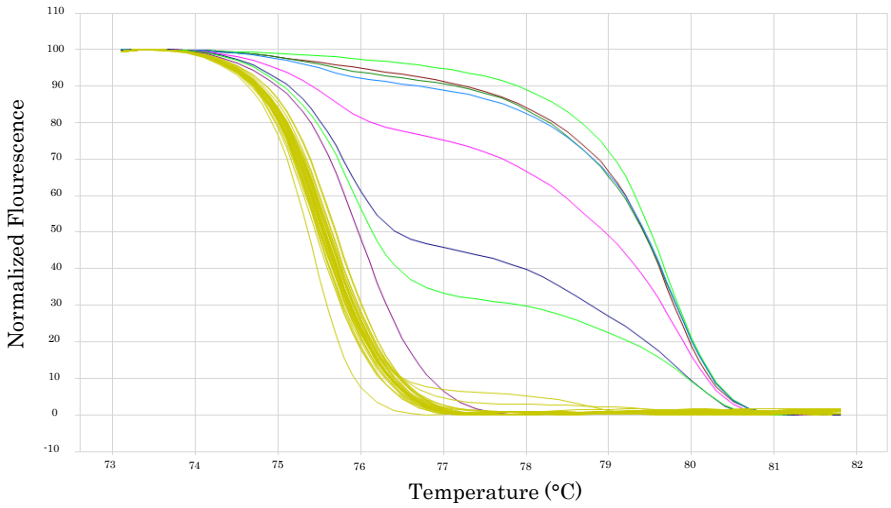

Figure 4.12. Melting curves of standards. Methylation level in % distinguished by different colours: - 100%, - 90%, - 75%, - 50%, - 35%, - 15%, - 0%. The yellow color represents analyzed samples

Table 4.13. MS-HRM master-mix and concentrations

Component	Volume/reaction (µl)
HRM Master Mix	5
Primer_forward (10µM)	0.3
Primer_reverse (10µM)	0.3
RNase-free water	3.4
Template (DNA/standard)	1

4.2.4 Cell culture techniques

Mammalian cells were manipulated according to the standard cell culture protocols Freshney (2005). Cells were cultivated in D-MEM (Dulbecco's modified Eagle's medium), supplemented with 10% fetal bovine serum and Penicillin (100 U/ml) – Streptomycin (100 ng/ml).

Neocarzinostatin (NCS) mediated DMA damage were examined in two ovarian cancer cell lines i) A2780 adherent ovarian *MLH1* – proficient cell line and ii) cisplatin-resistant cell line A2780/CP adherent ovarian *MLH1* –deficient cell line (caused by hypermethylation of the gene promoter).

Cells were kept at 37 °C under 5% CO_2 atmosphere. Cells were counted using Bürker counting chamber according to the standard protocol Freshney (2005). Asynchronic cells were plated in $1 \cdot 10^6$ per 10 cm plate, cells at 70% confluence. Following day, BrdU (bromodeoxyuridine) in a final concentration of 10 μM, and 1μM of Nocodazole (NDZ) were added to cell culture 1 hour before Neocarzinostatin treatment for causing DSBs. Medium with NCS was removed after 1 hour, and the cells were washed free of NCS. The BrdU is incorporated into newly synthetized DNA, thus indicating cells were in S-phase and NDZ treated cells arrest in G_2- or M-phase. The cell viability was determined by DAPI staining in concentration 1 ug/ml. Cells were harvested for FACS analysis and WB after 6 and 24 hours after NDZ treatment.

Cell harvest

Cells were washed with cold 1× PBS, and add cold cell lysis buffer with protease inhibitor cocktail. Incubate for 30 minutes on ice, and then centrifuged for 10 minutes at 12,000 RPM, at 4°C. Supernatant was transferred fresh tube and store at -20°C or -80°C. For FACS analysis, cells were washed with cold PBS and stored in 70% ethanol at 4°C.

4.2.5 Fluorescence-activated cell sorting (FACS) analysis of cell cycle

Alcohol-fixed cells were permeabilized (Triton X-100) for the intracellular staining. Cells treated with BrdU were stained with specific fluorescent anti-BrdU antibody conjugated with FITC. Nocodazol treated cells were utilized Anti

Histone H3 (pSer28)-Alexa Fluor® 647 as the pH3 antibody to investigate M phase. Incubations were followed with a set of washes with 1× PBS and spinning 300g/3min/4°C. For cell viability 4',6-Diamidino-2-Phenylindole (DAPI) was used.

In addition, cell cycle gates were adjusted to include G_0/G_1, S, and G_2/M populations. In summary, percentage of events in the cell gate, and percentage of cells in G_0/G_1, S, and G_2/M populations were evaluated from flow cytometry analysis. Single cell analysis software FlowJo (Tree Star) was used for analysing flow cytometry data.

4.2.6 Western blot

BCA assay

The total amount of protein in cell lysates was quantified using BCA assay to ensure identical loading in western blot Smith et al. (1985). The BCA assay was performed according to the manufacturer instructions. The concentration of protein using a spectrophotometer.

SDS-Polyacrylamide Gel Electrophoresis

SDS-Polyacrylamide Gel Electrophoresis (SDS-PAGE) was performed in the standard two-gel system developed by Laemmli (1970). Proteins were loaded on gradient gel and separated using electronic current on constant voltage. We used BioRad Mini-PROTEAN Tetra Cell apparatus.

The separated proteins were transferred from gel onto a nitrocellulose membrane through a wet transfer western blot. The gel/membrane sandwich was placed into buffer filled chamber; the western blot was run at constant voltage of 100 V for 1.5 hours. The quality of protein transfer was verified using Ponceau S staining of the membrane.

Before antibody is added, membrane was blocked in % [w/v] of nonfat dry milk in 1× PBS/0.05% Tween20 for 60 minutes. In the next step, the membrane was probed with specific primary antibody of the protein of our interest overnight at 4°C. Incubations were followed with a set of washes (1× PBS/0.05% Tween20), which helped non-specific antibody binding.

After washing out the unspecific binding, the membrane is incubated with secondary antibody for 1,5 hours, which recognises the primary antibody followed by series of washes. Final step was incubation of the membrane with mix of equal volume of chemiluminescent ECL reagent 1 and 2 and exposed to the medical X-ray film.

The western blot densitometry analysis was performed in ImageJ software (Abramoff et al., 2004; Rasband, 1997-201)1. No image adjustments were made prior to densitometry analysis. The results were normalized to the loading control (α-tubulin) from the same gel.

4.2.7 Statistical analysis

Statistically significant differences in the methylation levels were evaluated by non-parametric Mann-Whitney U test and in the gene expression evaluations were used One-Way test, Pearson test and Kolmogorov-Smirnov test. For cell cycle profile Two-Way ANOVA test was performed. The GenEx followed by the GeNorm and NormFinder software determined expression stability of the reference genes.

Statistical analyses were performed using the GraphPad Prism 4.0 (La Jolla, CA, USA). Differences were considered significant at $P \leq 0.05$.

5 Results

In this study, we analysed the set of 63 ovarian epithelial tumor samples and 12 healthy ovary tissues, that were collect within a project with PI Radka Václavíková, Ph.D. from The National Institute of Public Health; and collaboration of Prof. Lukáš Rob, M.D, Ph.D. from Motol University Hospital.

5.1 Validation and preparation of tools

In the beginning, we validated tools for further studies, especially panel of reference genes for the gene expression, specificity of mono/polyclonal antibodies binding MMR proteins. Moreover, designing methylation specific primers and their validation was needed.

5.1.1 Validation of housekeeping genes for gene expression

Ten reference genes were using for optimization of the expression stability in tumor ovarian samples and healthy tissue, namely *ACTB, GAPDH, UBC, B2M, YWHAZ, 18S, TOP1, EXO, HPRT, GUS.* One reference gene *PPIA* was selected on the basis of literature (Li *et al.*, 2009). The total RNA was isolated and cDNA reverse transcription was performed by following manufacture protocol, individual cDNA samples and a random pool of cDNA were used for optimization.

The GenEx software, employing geNORM and NormFinder normalization was used for data analysis and processing. We found that the expression of *UBC* and *YWHAZ* were constant in both tumors and healthy tissues. Finally, geNorm identified *GAPDH* and *YWHAZ* as the most stable expressed, while NormFinder indicated *UBC* with best stability (Figure 5.1).

Therefore, *UBC, YWHAZ,* and *PPIA* seem to be reliable for RT-qPCR analysis in ovarian cancer (Figure 5.1).

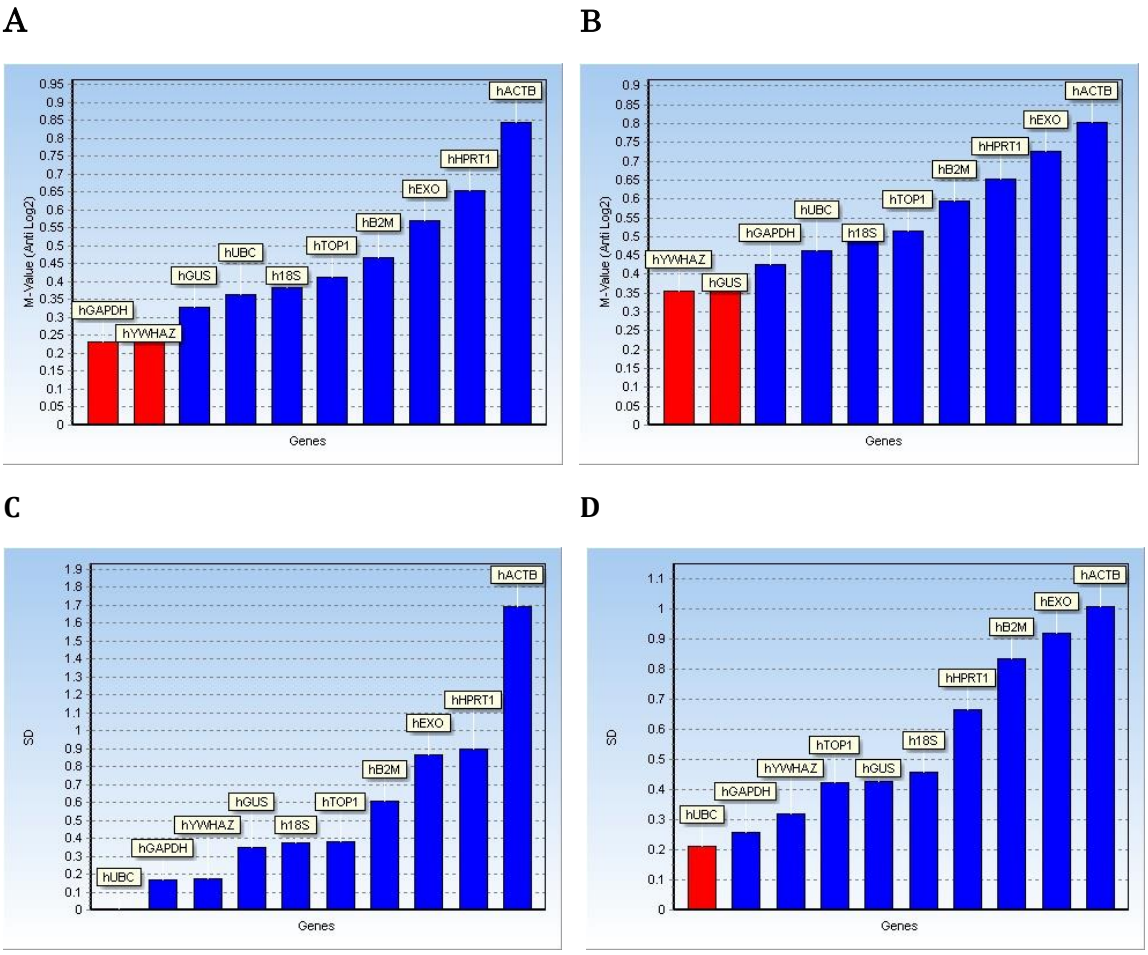

Figure 5.1. Reference genes optimisation. Expression levels of the most stable reference genes are represented in red colour A) B) Reference gene normalization using geNorm algorithm **C) D)** Reference gene normalization using NormFinder algorithm

5.1.2 Design and validation of MS-HRM

Primers specific for bisulfite-converted DNA were designed using Methyl Primer Express Software v1.0 (Thermo Fisher Scientific Inc., Waltham, USA). The sequence of the primer used is shown in Figure 5.2 and Table 5.3. The fluorescence was measured once per cycle to monitor template amplification. DNA melting curves were acquired by measuring the fluorescence during a linear temperature transition from 55 °C to 95 °C at 0.1 °C/s with initial denaturation started at 95°C for 15 s.

TTTAGTCGCGATTTTTTAAGGTTAAGAGGCGGTAGAGTTCGAGGTTTGTACGAGTAGTTTTTTTTTTAGGAG
TGAAGGAGGTTACGGGTAAGTCGTTTTGACGTAGACGTTTTATTAGGGTCGCGCGTTCGTCGTTCGTTATAT
ATCGTTCGTAGTATTCGTGTTTAGTTTCGTAGTGGCGTTTGACGTCGCGTTCGCGGGTAGTTACGATGAGGC
GGCGATAGATTAGGTATAGGGTTTTATCGTTTTTCGGAGGTTTTATTATTAAATAACGTTGGGTTTATTCGG
GTCGGAAAATTAGAGTTTCGTCGATTTTTATTTTGTTTTTTTTGGGCGTTATTTATATTTTGCGGGAGGTTA
TAAGAGTAGGGTTAACGTTAGAAAGGTCGTAAGGGGAGAGGAGGAGTTTGAGAAGCGTTAAGTATTTTTTTC
GTTTTGCGTTAGATTATTTTAGTAGAGGTATATAAGTTCGGTTTCGGTATTTTTGTTTTTATTGGTTGGATA
TTTCGTATTTTTCGAGTTTTTAAAAACGAATTAATAGGAAGAGCGGATAGCGATTTTTAACGCGTAAGCGTA
TATTTTTTTAGGTAGCGGGTAGTAGTCGTTTTAGGGAGGGACGAAGAGATTTAGTAATTTATAGAGTTGAGA
AATTTGATTGGTATTTAAGTTGTTTAATTAATAGTTGTCGTTGAAGGGTGGGGTTGGATGGCGTAAGTTATA
GTTGAAGGAAGAACGTGAGTACGAGGTATTGAGGTGATTGGTTGAAGGTATTTTCGTTGAGTATTTAGACGT
TTTTTTGGTTTTTTTGGCGTTAAAATGTCGTTCGTGGTAGGGGTTATTCGGCGGTTGGACGAGATAGTGGTG
AATCGTATCGCGGCGGGGGAAGTTATTTAGCGGTTAGTTAATGTTATTAAAGAGATGATTGAGAATTGGTAC
GGAGGGAGTCGAGTCGGGTTTATTTAAGGGTTACGATTTAACGGGTCGCGTTATTTAATGGCGCGGATACGT
TTTTTTGTTCGGGTAGAGGTATGTATAGCGTATGTTTATAACGGCGGAGGTCGTCGGGTTTTTTGACGTGTT
AGTTAGGTTTTTTTTTTTTTCGTAGATCGTGTGTTTTTTTATCGTTTTTTTTCGAGATTTTTTAAGGGTTGT
TTGGAGTGTAAGTGGAGGAATATACGTAGTGTTGTTTTAATGGTATCGTTAATTAAGTAAGGAAGTTATTTA
ATTTAAAATTATGTATGTAGAATATGCGAAGTTAAAAGATGTATAAAAGTTTAAGATGGGGAGAAAAATTTT
TTTTTAGAGGGTATTGTGTTATTGTTTTTTTGTTTTTTATTTATTTTAGAAATTATTTGTTTATATTTAAAG
GTATAATTTATTTTGAGTT

Figure 5.2. Primer design of *MLH1* Bisulfite convereted DNA for MS-HRM. The HRM primers are represented in green color

Table 5.3. The primer sequences used for MS-HRM

Primers	Sequence (5′–3′)	PCR product size (bp)
MLH1_forward	GAGTTGAGAAATTTGATTGGTATTT	124
MLH1_reverse	AACCAATCACCTCAATACCTC	

5.2 Estimation of expression profile of MMR genes in ovarian tumors and healthy control tissue

The expression profile of MMR genes was performed in the two-step process using florescent-labeled TaqMan® probes (Thermo Fisher Scientific Inc., Waltham, USA. First, the cDNA synthesis produced by reverse transcriptase was measured and diluted on 25 ng/µl in reaction. Second, the relative quantification of Ct was analyzed by using GeneEx programme.

We concluded that expression of mRNA of following genes *MLH1*, *MLH3*, *MSH3*, *MSH6*, *PMS1*, *PMS2* is down-regulated in tumor tissue compared to healthy controls, whereas, *MSH2* was the only gene up-regulated in tumors (Figures 5.4). There is also a high interindividual variability between samples

and among the groups. For statistical analysis of mRNA expression three tests were performed:

1. Kolmogorov-Smirnov test – significance ≥ 0.05 in all genes
2. One-Way ANOVA test – significance ≥ 0.05 in all genes
3. Pearson test - significance ≥ 0.05 in all genes

Based on the clinical data of patients, by comparing stages I+II and III+IV, we observed statistically significant up-regulation in genes *MSH2* (P≤0,032) in earlier stages (I+II), and *MLH1* (P ≤0.017), *PMS1* (P≤0,033) in the latter stages III+IV.

The comparison between mucinous serous ovarian tumor type with others such, serous, endometrioid, undifferentiated or unclassifiable revealed that statistically significant decrease in expression of gene *MLH1* (P ≤0.032) in the high grade serous ones.

In samples with elevated Ki67 proliferation marker (> 13%) we observed *MLH1* down-regulation (P ≤ 0,033) indicating that increased expression of Ki67 correlates with decreased *MLH1* expression.

Three candidate genes were selected, *MLH1*, *MSH2*, and *PMS1,* on the basis of clinical features of the patient.

MLH1 gene – with higher tumor grade the *MLH1* expression decreases; in respect to serous ovarian tumors (the highest grade) were the *MLH1* expression was significantly lower.

MSH2 gene – the *MSH2* expression is down regulated in tumor samples with positive CA125 marker and before ovary surgery with respect to end of the chemotherapy.

PMS1 gene – *PMS1* expression decreases with increasing tumor grade and disease progression; the. *PMS1* is related to grade and disease progression.

In conclusion, two candidate genes *MLH1* and *MSH2* were selected for further detailed studies. Protein level analysis (Table 5.5) was further performed on tissue samples from patients with highest and lowest mRNA expression.

A

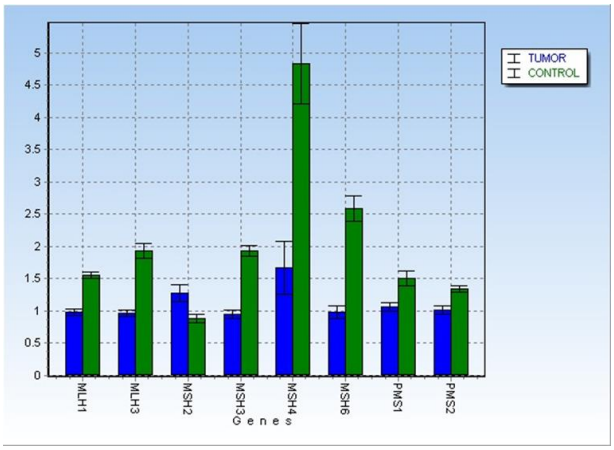

B

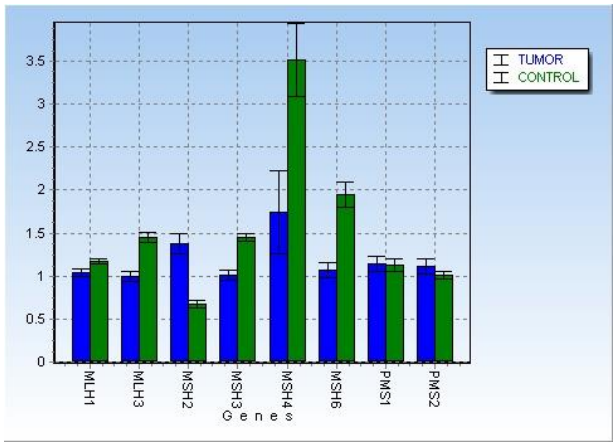

C

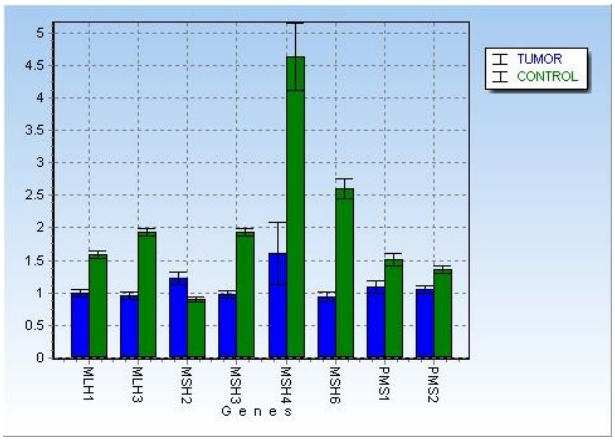

Figure 5.4. Relative MMR gene expression. All MMR genes are down-regulated in tumor samples expect *MSH2*, where is up-regulation in tumor compared to healthy tissue. Statistically no significant A) Relative MMR gene expression using *PPIA* as a reference gene **B)** the *UBC* served as the reference gene **C)** the *YHWAZ* served as the reference gene.

Table 5.5. Individual patients with highest and lowest mRNA expressions of *MLH1*, *MSH2* and *PMS1*. R=sample source identification; Number= patient order in database; T=tumor

Gene	Highest mRNA expression	Lowest mRNA expression
MLH1	R55T	R6T
	R62T	R76T
	R90T	R33T
MSH2	R55T	R22T
	R38T	R4T
	R43T	R6T
PMS1	R55T	R33T
	R61T	R15T
	R53T	R4T

5.3 Detection of MLH1 and MSH2 protein levels

Based on the mRNA expression data, we have focused on the protein analysis by using western blot of MLH1 and MSH2 in patients with most pronounced decrease in mRNA levels. Protein analysis was performed on patients with highest MLH1 or MSH2 mRNA level and the lowest (Table 5.6).

Table 5.6.Protein analysis based on the highest and lowest mRNA expressions of MLH1, and MSH2. R=sample source identification; Number= patient order in database; T=tumor

Gene	Highest mRNA expression	Lowest mRNA expression
MLH1	R55T	R6T
	R62T	R76T
	R90T	R33T
MSH2	R55T	R22T
	R38T	R4T
	R43T	R6T

We could not evaluate properly these results and further investigation is warranted. Ponceau staining of loaded protein in MLH1 seems to be at the same concentration, but the specificity of α-tubulin have not detected the same protein amount. We could not evaluate properly these results and further investigation is warranted. Similarly, the protein loading and antibody specificity was not satisfactory for MSH2 protein either (Figure 5.7).

In conclusion, these results indicate high intra-individual variability among patients that might be associated with the different disease stage, tumor grade and type as well as several different therapies and treatments.

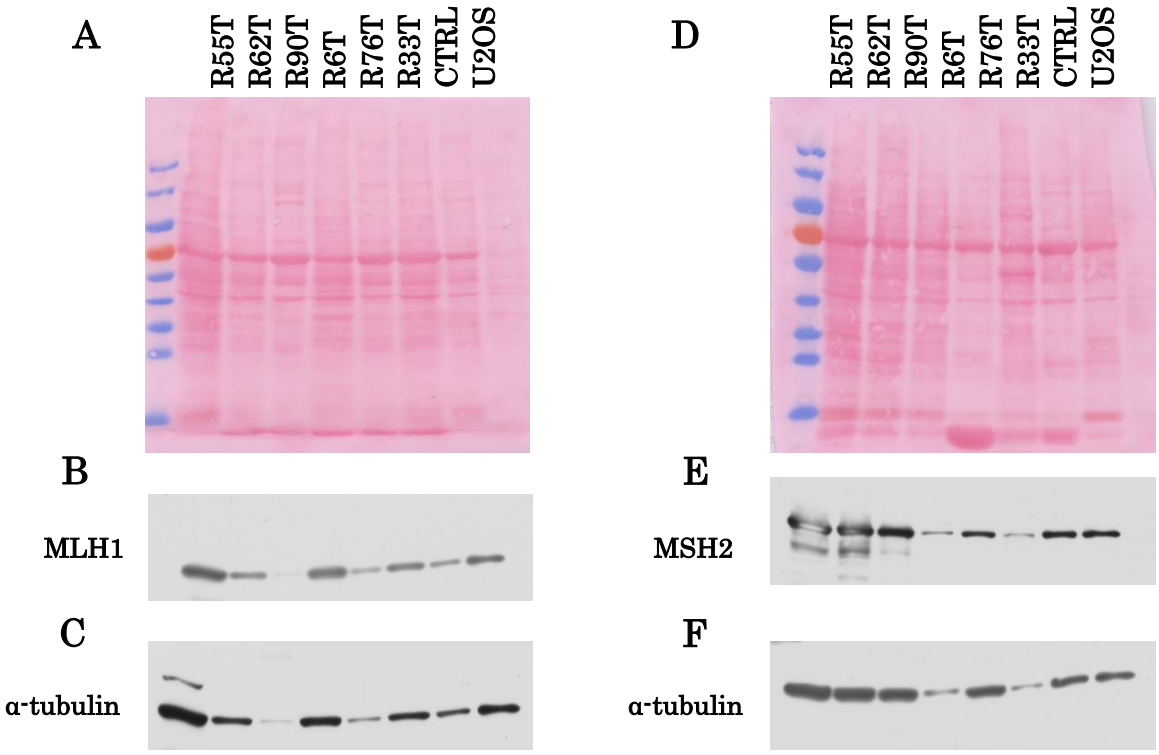

Figure 5.7. Protein expression of MLH1 and MSH2 in ovarian tumors and healthy tissue – A) Ponceau staining of protein loading control for MLH1 **B)** Protein levels of MLH1 in patients with highest and lowest mRNA expression **C)** α-tubulin staining as loading control **D)** Ponceau staining of MSH2 protein level **E)** Protein levels of MSH2 in patients with highest and lowest mRNA expression **F)** α-tubulin loading control

5.4 Determination promoter methylation status of MMR genes

In this study, the level of *MLH1* promoter methylation was determined by using MS-HRM method. Genomic DNA was isolated using DNeasy® Blood & Tissue kit (Qiagen, Venlo, Netherlands) following bisulfite conversion. This treatment enables to deaminate unmethylated cytosine to produce uracil in

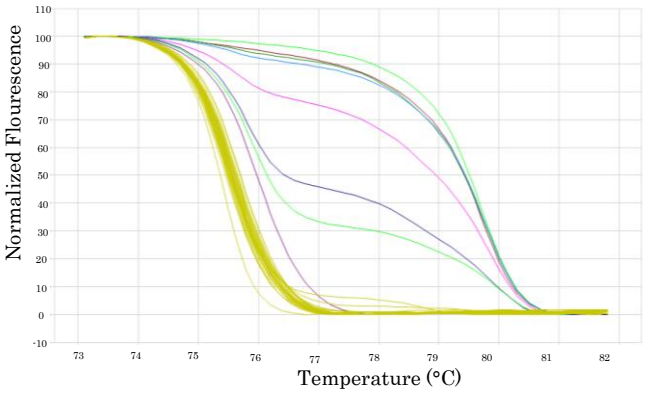

Figure 5.8. Methylation status of MLH1 promoter in ovarian tumors. The standards are represented by colors - 100, 75, 50, 35, 25, 10, 5, 0 % and the analysed samples by yellow colour

DNA. Methylated cytosines are protected from the conversion to uracil, allowing determining unmethylated cytosines and 5-methylcytosines. A set of primers was designed for promoter region of the *MLH1* gene and the optimal conditions for MS-HRM were set up. PCR products were verified by gel electrophoresis using 1.5% of agar gel.

Table 5.9. The percentage of *MLH1* methylation status in epithelial ovarian tumors (black) and ovary healthy tissue (green).

Tumor	No. Patient	MLH1 %	Tumor	No. Patient	MLH1 %	Healthy tissue	No. Control	MLH1 %
T	95	0	T	128	0	K	1	0
T	96	0	T	131	0	K	2	0
T	97	0	T	132	0	K	3	0
T	98	0	T	136	0	K	4	0
T	99	0	T	137	0	K	5	0
T	100	0	T	138	0	K	6	0
T	101	0	T	141	0	K	7	0
T	102	0	T	142	0	K	8	0
T	105	0	T	143	0	K	9	0
T	107	0	T	145	0	K	10	0
T	109	0	T	146	0	K	11	0
T	110	0	T	149	0	K	12	0
T	111	0	T	150	0			
T	112	0	T	151	0			
T	113	0	T	153	0			
T	114	0	T	154	0			
T	115	0	T	155	0			
T	116	0	T	156	0			
T	117	0	T	157	0			
T	118	0	T	158	0			
T	119	0	T	159	0			
T	121	0	T	160	0			
T	122	0	T	162	0			
T	123	0	T	163	0			
T	125	0	T	164	0			

In all samples, there was no evidence of increased *MLH1* promoter methylation level (0% in all samples tested for methylation status) (Figure 5.8, Table 5.9).

In conclusion, our set of tumor and control may not be sufficiently large to disclose the aberrant methylation status.

5.5 Analysis of cell cycle progression after DNA damage

To clarify the role of *MLH1* in cell cycle progression, we compared two ovarian cell lines i) *MLH1* proficient cell line called A2780 and ii) *MLH1* deficient cisplatin resistant ovarian cell line called A2780/CP.

We compared the cell response to DNA damage after 6 and 24 hours, suggesting that *MLH1* deficiency affect the cell progression and cell will be arrested in G_2 phase due to incomplete replication.

Cell lines with damage agent arrested in the G_2 compared to non-treated control cells, with significant difference between *MLH1* proficient and deficient cells (35% vs. 42%, $P \leq 0.05$). The G_2 arrest was increased 6 hours after damage in both cell lines compared to 24-hour time point. After 24 hours treated cells showed same cell cycle pattern as control cells. The decreased G_2 arrest in *MLH1* proficient cells (A2780) compared to those deficient (A2780/CP) (35% vs.46%, $P \leq 0.01$) suggest *MLH1* importance in DNA damage induced replication stress (Figure 5.10).

The comparison between the 6 hour and 24 hour time point was significantly decreased of G_2 cells after 24h, suggesting that cell undergo the check point recovery. The A2780 *MLH1* proficient ovarian cell line with shows decrease from 35 % in 6 hours to 16% in 24 hours after damage ($P \leq 0.01$), in A2780/CP *MLH1* deficient cells we observed similar pattern of decrease from 42% to 9% ($P \leq 0.01$) (Figure 5.11).

The number of cells in M phase has significantly increased (4.0% vs. 8.0% $P \leq 0.01$) between cell lines in 6h time point (Figure 5.12), suggesting that cells are exposed to continual replication stress or they undergo apoptosis. More importantly, we have not observed differences in treated and non-treated cells in M phase after G_2 check point arrest regardless of any experimental condition.

A

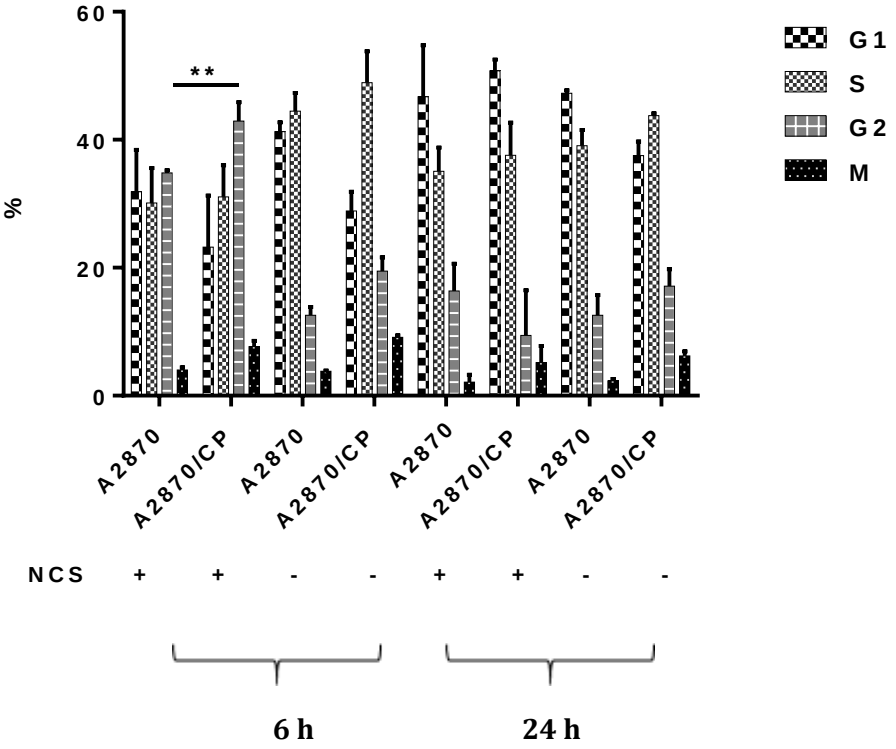

B

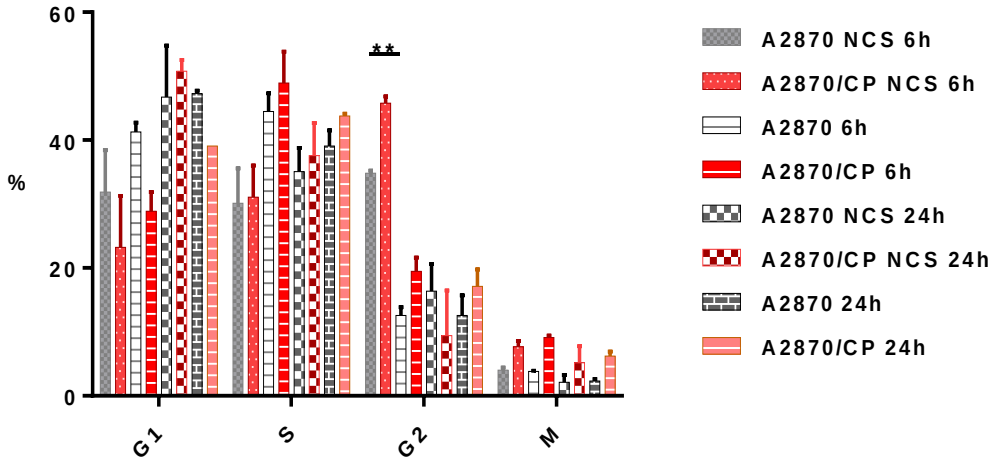

Figure 5.10. Comparison of cell cycle profile between two ovarian cell lines 6h and 24h after damage. A2780 cell line is MLH1 proficient and A2780/CP is MLH1 deficient A) Cell cycle progression **B)** Statistical significance ($P<0.05$) in G_2 phase between both cell line 6h after DNA damage occurred

A

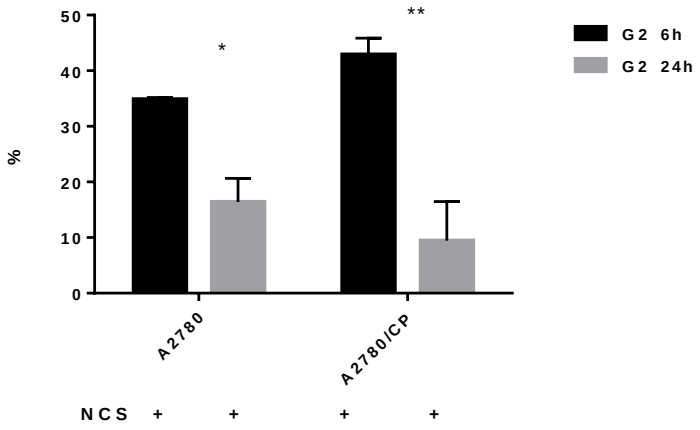

B

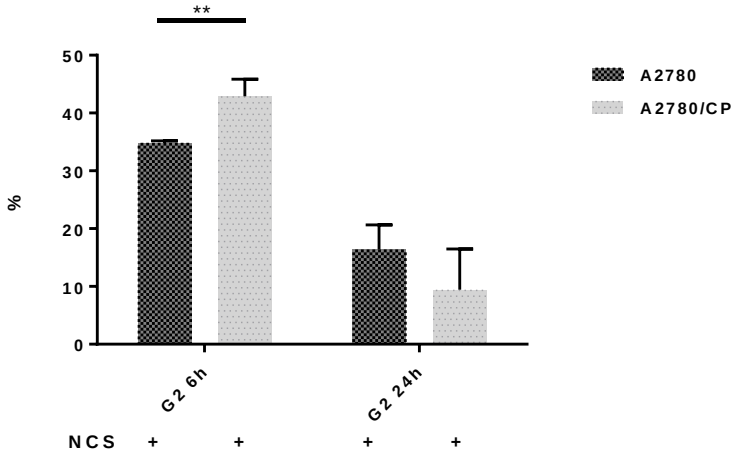

Figure 5.11. G_2 cell cycle analysis of two ovarian cell lines A2780 - *MLH1* proficient and A2780/CP – *MLH1* deficient cell lines. A) Flow Cytometer analysis showed G_2 arrest after DNA damage in both cell lines after 6h **B)** Comparison of 6h and 24h difference in G_2 after damage in each cell line P <0.001

A

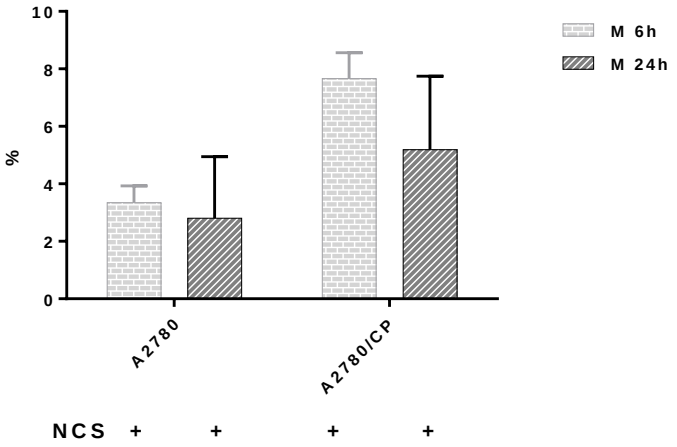

B

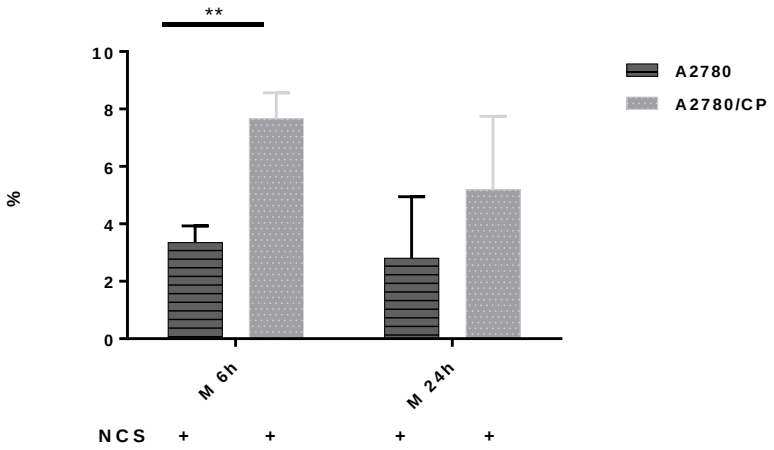

Figure 5.12. the M cell cycle analysis of two ovarian cell lines A2780 - *MLH1* proficient and A2780/CP – *MLH1* deficient cell lines M cell cycle analysis A) B) Detailed analysis of M phase after DNA damage

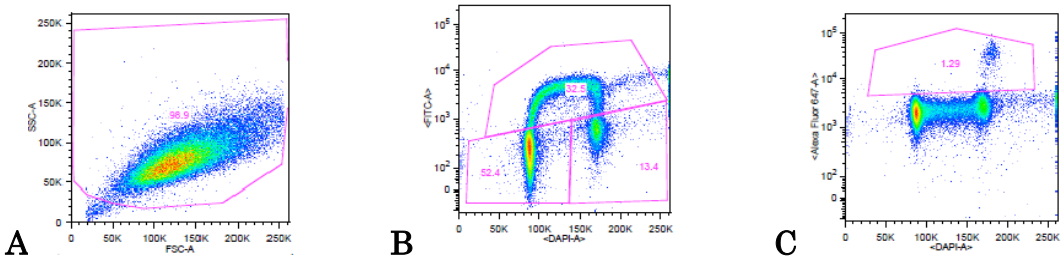

Figure 5.13. Flow Cytometry analysis of cell lines. A) SSC-A vs. FSC-A indicates singlets gating **B)** FITC vs. DAPI indicates G1, S and G_2 phases **C)** Alexa 647 vs. DAPI indicates pH3 staining for M phase

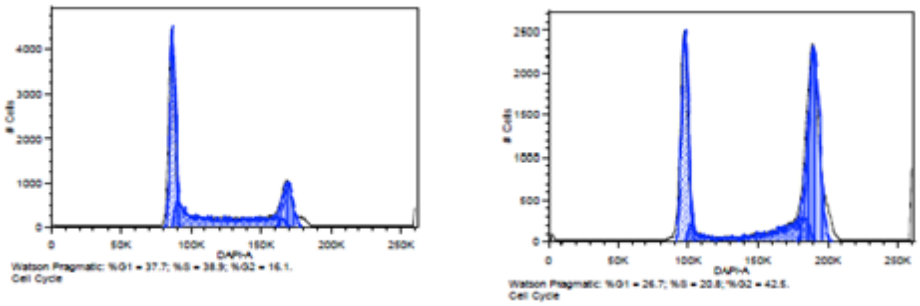

Figure 5.14. Cell cycle histogram. First peak represents G_1 phase, following S phase and second peak represents G_2

5.6 Detection of MLH1 and MSH2 protein levels in cell lines

To investigate whether depletion of *MLH1* has an influence on MMR heterodimer partners, we performed western blot analysis for detection of MSH2 and PMS1. We prepared cell lysates from A2780, A2780/CP and MCF7 (antibody specificity binding control). Protein expression of MSH2 could be detected in the same level in the cell lines and all experimental conditions. No difference in protein level was observed in both 6h and 24h after DNA damage (Figure 5.15).

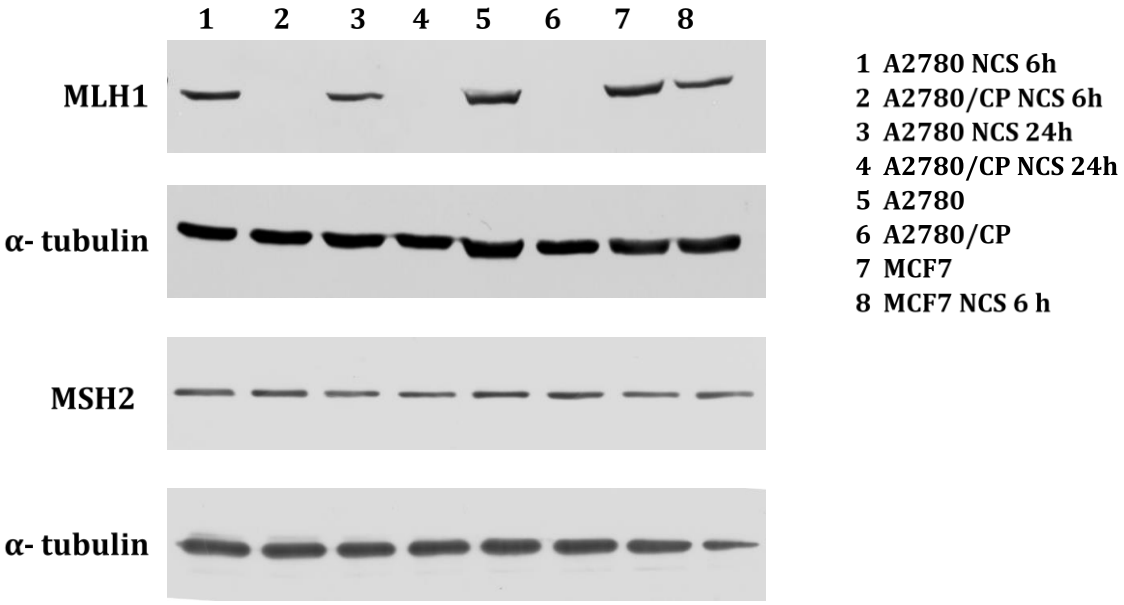

Figure 5.15. Protein levels measured after neocarzinostatin mediated DNA damage.

6 Discussion

To understand the importance of mismatch repair pathway and MLH1 status in the ovarian carcinogenesis, we have investigated the role of MMR gene expressions, epigenetic alteration of MLH1, cell cycle progression in the cellular model systems with an ultimate goal to identify the link between MMR and malignant transformation and cancer progression.

Recently, approximately in 6% of the cases abnormal function in MMR genes was identified with regard to epithelial ovarian tumors (Bennett *et al.*, 2016). More specifically, over 31% of cases exhibited a loss of expression in MMR genes (Kobayashi *et al.*, 2015). On the bases of our data set we have recorded down-regulation of the majority of MMR genes in tumors except for *MHS2* that is up-regulated in tumors. However, we have not observed a total loss of expression. Surprisingly, we noted the highest mRNA expressions of *MLH1*, *MSH2* and *PMS1* in one patient, most likely in correlation with individual tumor characteristics, based on the stage and grade. Concerning clinical data, our data also showed relevance of up-regulation of *MLH1*, *MSH2* and *PMS1* with tumor type and grade. The *MLH1* might be correlated with higher tumor grade where we consistently observed significant increase in expression. In recent studies, the authors observed significantly increased levels of *MSH3* gene expression in tumor colonic tissue in comparison with non-neoplastic tissues. Interestingly, all of the MMR genes were expressed differentially in dependance on the location of the tumor. Especially colon cancer showed increased *MSH2*, *MSH3*, *MSH6* and *PMS2* gene expression compared to rectal tumors ($p = 0.02$) (Vymetalkova *et al.,* 2014). Additionally, in our study (or in our hands) the MLH1 and MSH2 protein did not correlate with mRNA expression due to technical problem of loading control or due to high tissue variability.

These, although somehow controversial, results could confirm the important consideration of correlation between the tumor stage distributions and tumor location. Therefore, the study population has to be optimally representative of exact tumor location. Unfortunately, our clinical data was

lacking this particular information and this direction might be interesting for further studies.

On a basis of obtained data we may ask a question, whether apparent down-regulation of MMR genes may be also due to epigenetic mechanism, such as methylation of promoter regions of individual genes. As shown in the literature (Okugawa et al., 2015), gene silencing through promoter methylation can cause MMR genes dysfunction. Up to now, Shilpa and co-authors showed promoter methylation status in *MLH1*, *MSH2,* and *PMS2* where the promoter of *MLH1* was methylated in 37.5% cases, *MSH2* in 8% and *PMS2* in one out of 87 patient with ovary tumor (Shilpa *et al.*, 2014). We evaluated 63 ovarian tumors and 12 healthy referent tissues to disclose information about *MLH1* hypermethylation status. Hence, our results do not support published data, since we did not discover any increased levels of *MLH1* promoter methylation. None of the cases showed aberrant methylation in *MLH1* gene. The general limitation of several studies was that tumor samples from patients were compared to a small number healthy donors what might be an additional cause of variability, including our study. Another reason may be a high intra-individual variation and group diversity due to the tumor grade, ethnicity, age, and treatment prior to the study. However, more knowledge is emerging on the topic of tumor heterogeneity, which may grossly impact the outcomes from various studies.

We also performed model *in vitro* experiments on appropriate cell lines (for details see Materials and Methods) to understand the role of *MLH1* as a candidate gene in molecular mechanism underlying ovarian carcinogenesis. In our study, we used two epithelial ovarian cell lines, the MLH1 proficient and deficient, to determine whether *MLH1* is involved in neocarzinostatin (NCS)-mediated DNA damage and mediates a response in G_2 arrest. We show that MMR, particularly *MLH1*, might be involved in regulation of G_2 cell cycle check-point by extending the G_2 arrest. Both cells lines were arrested in G_2 phase 6 hours after the damage, what might be the consequence of incomplete replication. The *MLH1* deficient cells were significantly ($P<0.01$) more arrested in G_2 phase; in accord with general belief that a *MLH1* proficient cells had an

ample time and capacity to repair the DNA damage prior to the entering to M, as compared to deficient ones which need longer time to go over. In contrast to our observation, it was previously reported that *MLH1*-deficient human colon carcinoma HCT116 cells as well as A2780/CP cells demonstrated reduced and shorter G_2 arrest as a response to irradiation (Yan *et. al.*, 2001). This observation is in concordance with the assumption that G_2 arrest is triggered by multiple mechanisms, and depending on the type of the damage.

Surprisingly, the M phase has similar progression pattern between treated and non-treated cells, whereas the cells with *MLH1* deficiency show unexpectedly increased % of cells in M phase compared to proficient cells at both time points. On the other hand, the M phase of the *MLH1* deficient cells are at the same level irrespective of DNA damage condition. This observation can be explained that cells with lack of ability to arrest in G_2 subsequently die.

With this knowledge we looked at the presence of other MMR gene, MSH2, for support to a more direct role in G_2 arrest. The MSH2 expression seemed to be identical in MMR- deficient and proficient tumor cell lines as well as in those treated versus non-treated. The comparable results were observed in colon carcinoma HCT116 ($MLH1^-$) (Yan *et. al.*, 2001) with no increased MSH2 expression after DNA damage induced by IR.

In summary, our result show that MMR might play the role in G_2 arrest response after DNA damage and raise a demand for further studies on how MMR participate in DNA damage response by regulating G_2/M progression in ovarian (and perhaps other malignancies as well) cancer. From the clinical point of view, MMR pathway might be regulated also by additional pathways, such as miRNA regulation, mutation based microsatellite instability, single nucleotide polymorphisms etc. Increased progress in this field suggests that MMR defects could play an important role in tumor development, including ovary.

7 Conclusions

The Diploma Thesis deals with the monitoring of mismatch repair genes in the pathogenesis of ovarian cancer, with following aims and conclusion.

- **Estimation of mRNA expression profile of MMR genes**

  The expression profile of MMR genes, namely *MLH1*, *MLH3*, *MSH3*, *MSH6*, *PMS1*, *PMS2* , were analyzed on set of 63 ovarian tumors and 12 healthy ovary tissues. All genes were down-regulated in tumors, except for *MSH2* exhibiting an up-regulation in tumors compared to healthy tissue. We selected two candidate genes (*MLH1* and *MSH2*) for further investigation. We observed unambiguous correlation of MMR genes with grade and type of tumors

- **Analysis of *MLH1* promoter methylation**

  The promoter methylation status was analyzed on the same set of samples. We have not detected any increased methylation level in promoter region of *MLH1* candidate gene. In conclusion: the down-regulation of *MLH1* might be due to other regulation mechanisms, such as miRNA protein degradation.

- **Detection of protein levels of MMR proteins**

  The level of candidate proteins in patient samples are not conclusive due to i) large heterogeneity of the samples based on tumor grade, type, therapy, ii) or due to technical error on western blot method

- **Estimation the role of *MLH1* in ovarian cancer cell lines**

  We investigated the importance of *MLH1* throughout cell cycle progression following DNA damage. *MLH1* might have a role in G_2 check point arrest. *MLH1* deficient cell are significantly more frequently arrested at G_2 phase as compared to *MLH1* proficient cells.

  .

8 Bibliography

ABRAMOFF, M., MAGALHAES, P., RAM, S. 2004 Image Processing with ImageJ. Biophotonics International 11: 36–42.

ABU-SANAD, A., Y. WANG, F. HASHEMINASAB, J. PANASCI, A. NOE *et al.*, 2015 Simultaneous inhibition of ATR and PARP sensitizes colon cancer cell lines to irinotecan. Front Pharmacol **6:** 147.

ALBARAKATI, N., T. M. ABDEL-FATAH, R. DOHERTY, R. RUSSELL, D. AGARWAL *et al.*, 2015 Targeting BRCA1-BER deficient breast cancer by ATM or DNA-PKcs blockade either alone or in combination with cisplatin for personalized therapy. Mol Oncol **9:** 204-217.

AMBROSE, M., and R. A. GATTI, 2013 Pathogenesis of ataxia-telangiectasia: the next generation of ATM functions. Blood **121**: 4036-4045.

ARAMA, M. E., and T. A. KUNKEL, 2010 Mutator phenotypes due to DNA replication infidelity. Semin Cancer Biol **20**: 304-311.

BEGUM, R., and S. A. MARTIN, 2016 Targeting Mismatch Repair defects: A novel strategy for personalized cancer treatment. DNA Repair (Amst) 38: 135-139.

BELANGER, F., J. P. ANGERS, E. FORTIER, I. HAMMONF-MARTEL, S. CONSTANTINO *et al.*, 2016 Mutations in Replicative Stress Response Pathways Are Associated with S Phase-specific Defects in Nucleotide Excision Repair. J Biol Chem **291**: 522-537.

BENADA, J., and L. MACUREK, 2015 Targeting the Checkpoint to Kill Cancer Cells. Biomolecules **5**: 1912-1937.

BENNETT, J. A., V. MORALES-OYARVIDE, S. CAMPBELL, T. A. LONGACRE and E. OLIVA, 2016 Mismatch Repair Protein Expression in Clear Cell Carcinoma of the Ovary: Incidence and Morphologic Associations in 109 Cases. Am J Surg Pathol.

BISCHOF, O., S. H. KIM, J. IRVIN, S. BERESTEN, N. A. ELLIS *et al.*, 2001 Regulation and localization of the Bloom syndrome protein in response to DNA damage. J Cell Biol **153**: 367-380.

BOTTONI, P., and R. SCATENA, 2015 The Role of CA 125 as Tumor Marker: Biochemical and Clinical Aspects. Adv Exp Med Biol **867:** 229-244.

CALDECOTT, K. W., 2008 Single-strand break repair and genetic disease. Nat Rev Genet **9:** 619-631.

COSTANTINO, L., S. K. SOTIRIOU, J. K. RANTALA, S. MAGIN, E. MLADENOV *et al.*, 2014 Break-induced replication repair of damaged forks induces genomic duplications in human cells. Science **343:** 88-91.

CURRADI, M., A. IZZO, G. BADARACCO and N. LANDSBERGER, 2002 Molecular mechanisms of gene silencing mediated by DNA methylation. Mol Cell Biol **22:** 3157-3173.

DIKMEN, Z. G., A. COLAK, P. DOGAN, S. TUNCER and F. AKBIYIK, 2015 Diagnostic performances of CA125, HE4, and ROMA index in ovarian cancer. Eur J Gynaecol Oncol **36:** 457-462.

DURATURO, F., R. LICCARDO, A. CAVALLO, M. DE ROSA, G. B. ROSSI *et al.*, 2015 Multivariate analysis as a method for evaluating the pathogenicity of novel genetic MLH1 variants in patients with colorectal cancer and microsatellite instability. Int J Mol Med **36:** 511-517.

EUSTERMANN, S., W. F. WU, M. F. LANGELIER, J. C. YANG, L. E. EASTON *et al.*, 2015 Structural Basis of Detection and Signaling of DNA Single-Strand Breaks by Human PARP-1. Mol Cell **60:** 742-754.

FARKAS, S., V. VYMETALKOVA, L. VODICKOVA *et al.*, 2014 DNA methylation changes in genes frequently mutated in sporadic colorectal cancer and in the DNA repair and Wnt/ß-catenin signaling pathway genes. Epigenomics **6**: 179-191.

FRESHNEY, R. I., 2005 Culture of Animal Cells: A Manual of Basic Technique. Wiley.

FRIEDHOFF, P., P. LI and J. GOTTHARDT, 2016 Protein-protein interactions in DNA mismatch repair. DNA Repair (Amst) **38:** 50-57.

GAO, D., J. G. HERMAN and M. GUO, 2016 The clinical value of aberrant epigenetic changes of DNA damage repair genes in human cancer. Oncotarget.

GROOTHUIZEN, F. S., and T. K. SIXMA, 2016 The conserved molecular machinery in DNA mismatch repair enzyme structures. DNA Repair (Amst) **38:** 14-23.

HARALDSDOTTIR, S., H. HAMPEL, C. WU, D. Y. WENG, P. G. SHIELDS *et al.*, 2016 Patients with colorectal cancer associated with Lynch syndrome and MLH1 promoter hypermethylation have similar prognoses. Genet Med.

HASSEN, S., A. A. ALI, S. P. KILAPARTY, Q. A. AL-ANBAKY, W. MAJEED *et al.*, 2016 Interdependence of DNA mismatch repair proteins MLH1 and MSH2 in apoptosis in human colorectal carcinoma cell lines. Mol Cell Biochem **412:** 297-305.

HELLEDAY, T., S. ESHTAD and S. NIK-ZAINAL, 2014 Mechanisms underlying mutational signatures in human cancers. Nat Rev Genet **15:** 585-598.

HEMMINKI, K., L. AALTONEN, X.LI, 2003 Subsequent primary malignancies after endometrial carcinoma and ovarian carcinoma. Cancer **97**: 2432-2439.

HINGORANI, M. M., 2016 Mismatch binding, ADP-ATP exchange and intramolecular signaling during mismatch repair. DNA Repair (Amst) **38:** 24-31.

HOULLEBERGHS, H., M. DEKKER, H. LANTERMANS, R. KLEINENDORST, H. J. DUBBINK *et al.*, 2016 Oligonucleotide-directed mutagenesis screen to identify pathogenic Lynch syndrome-associated MSH2 DNA mismatch repair gene variants. Proc Natl Acad Sci U S A.

ILIAKIS, G., T. MURMANN and A. SONI, 2015 Alternative end-joining repair pathways are the ultimate backup for abrogated classical non-homologous end-joining and homologous recombination repair: Implications for the formation of chromosome translocations. Mutat Res Genet Toxicol Environ Mutagen **793:** 166-175.

JEFFRIES, E. P., W. H. DENQ, J. C. BARTKO and M. A. TRAKSELIS, 2013 Identification, quantification, and evolutionary analysis of a novel isoform of MCM9. Gene **519:** 41-49.

JEGGO, P. A., and M. LOBRICH, 2015 How cancer cells hijack DNA double-strand break repair pathways to gain genomic instability. Biochem J **471:** 1-11.

JEON, Y., D. KIM, J. V. MARTIN-LOPEZ, R. LEE, J. OH *et al.*, 2016 Dynamic control of strand excision during human DNA mismatch repair. Proc Natl Acad Sci U S A **113:** 3281-3286.

JIRICNY, J., 2013 Postreplicative mismatch repair. Cold Spring Harb Perspect Biol **5:** a012633.

KADYROVA, L. Y., and F. A. KADYROV, 2016 Endonuclease activities of MutLalpha and its homologs in DNA mismatch repair. DNA Repair (Amst) **38:** 42-49.

KANU, N., T. ZHANG, R. A. BURRELL, A. CHAKRABORTY, J. CRONSHAW *et al.*, 2015 RAD18, WRNIP1 and ATMIN promote ATM signalling in response to replication stress. Oncogene.

KIDAMBI, T. D., A. BLANCO, J. VAN ZIFFLE and J. P. TERDIMAN, 2016 Constitutional MLH1 methylation presenting with colonic polyposis syndrome and not Lynch syndrome. Fam Cancer **15:** 275-280.

KNITTEL, G., P. LIEDGENS and H. C. REINHARDT, 2015 Targeting ATM-deficient CLL through interference with DNA repair pathways. Front Genet **6:** 207.

KOBAYASHI, Y., K. NAKAMURA, H. NOMURA, K. BANNO, H. IRIE *et al.*, 2015 Clinicopathologic analysis with immunohistochemistry for DNA mismatch repair protein expression in synchronous primary endometrial and ovarian cancers. Int J Gynecol Cancer **25:** 440-446.

KURFURSTOVA, D., J. BARTKOVA, R. VRTEL, A. MICKOVA, A. BURDOVA *et al.*, 2016 DNA damage signalling barrier, oxidative stress and treatment-relevant DNA repair factor alterations during progression of human prostate cancer. Mol Oncol.

KWOK, M., N. DAVIES, A. AGATHANGGELOU, E. SMITH, C. OLDREIVE *et al.*, 2016 ATR inhibition induces synthetic lethality and overcomes chemoresistance in TP53- or ATM-defective chronic lymphocytic leukemia cells. Blood **127:** 582-595.

LAEMMLI, U. K., 1970 Cleavage of structural proteins during the assembly of the head of bacteriophage T4. Nature **227:** 680-685.

LAFRANCE-VANASSE, J., G. J. WILLIAMS and J. A. TAINER, 2015 Envisioning the dynamics and flexibility of Mre11-Rad50-Nbs1 complex to decipher its roles in DNA replication and repair. Prog Biophys Mol Biol **117:** 182-193.

LEYNS, L., and L. GONZALEZ, 2012 *Genomic Integrity of Mouse Embryonic Stem Cells*. INTECH Open Access Publisher.

LI, Y. L., F. YE, Y. HU, W. G. LU and X. XIE, 2009 Identification of suitable reference genes for gene expression studies of human serous ovarian cancer by real-time polymerase chain reaction. Anal Biochem **394:** 110-116.

LIEBER, M. R., 2010 NHEJ and its backup pathways in chromosomal translocations. Nat Struct Mol Biol **17:** 393-395.

LOZADA, E., J. YI, J. LUO and D. K. ORREN, 2014 Acetylation of Werner syndrome protein (WRN): relationships with DNA damage, DNA replication and DNA metabolic activities. Biogerontology **15:** 347-366.

MARECHAL, A., and L. ZOU, 2013 DNA damage sensing by the ATM and ATR kinases. Cold Spring Harb Perspect Biol **5**.

MCCABE, M. T., J. C. BRANDES and P. M. VERTINO, 2009 Cancer DNA methylation: molecular mechanisms and clinical implications. Clin Cancer Res **15:** 3927-3937.

F2015 Detection of DNA mismatch repair (MMR) deficiencies by immunohistochemistry can effectively diagnose the microsatellite instability (MSI) phenotype in endometrial carcinomas. Gynecol Oncol **137:** 306-310.

MINOCHERHOMJI, S., S. YING, V. A. BJERREGAARD, S. BURSOMANNO, A. ALELIUNAITE *et al.*, 2015 Replication stress activates DNA repair synthesis in mitosis. Nature **528:** 286-290.

MLADENOV, E., S. MAGIN, A. SONI and G. ILIAKIS, 2016 DNA double-strand-break repair in higher eukaryotes and its role in genomic instability and cancer: Cell cycle and proliferation-dependent regulation. Semin Cancer Biol.

OKUGAWA, Y., W.M. GRADY, A. GOEL 2015 Epigenetic Alterations in Colorectal Cancer: Emerging Biomarkers. Gastroenterology **149**:1204-1225.

PENA-DIAZ, J., and L. J. RASMUSSEN, 2016 Approaches to diagnose DNA mismatch repair gene defects in cancer. DNA Repair (Amst) **38:** 147-154.

POMMIER, Y., C. REDON, V. A. RAO, J. A. SEILER, O. SORDET *et al.*, 2003 Repair of and checkpoint response to topoisomerase I-mediated DNA damage. Mutat Res **532:** 173-203.

PRAKASH, R., Y. ZHANG, W. FENG and M. JASIN, 2015 Homologous recombination and human health: the roles of BRCA1, BRCA2, and associated proteins. Cold Spring Harb Perspect Biol **7:** a016600.

PRAT, J., and F. C. O. G. ONCOLOGY, 2015 FIGO's staging classification for cancer of the ovary, fallopian tube, and peritoneum: abridged republication. J Gynecol Oncol **26:** 87-89.

RAHMANIAN, S., R. TALEEI and H. NIKJOO, 2014 Radiation induced base excision repair (BER): a mechanistic mathematical approach. DNA Repair (Amst) **22:** 89-103.

RASBAND, W. (1997-2011.): ImageJ. http://imagej.nih.gov/ij/.

RIVERA-CALZADA, A., L. SPAGNOLO, L. H. PEARL and O. LLORCA, 2007 Structural model of full-length human Ku70-Ku80 heterodimer and its recognition of DNA and DNA-PKcs. EMBO Rep **8:** 56-62.

SAHNANE, N., F. MAGNOLI, B. BERNASCONI, M. G. TIBILETTI, C. ROMUALDI *et al.*, 2015 Aberrant DNA methylation profiles of inherited and sporadic colorectal cancer. Clin Epigenetics **7:** 131.

SAKATO, M., M. O'DONNELL and M. M. HINGORANI, 2012a A central swivel point in the RFC clamp loader controls PCNA opening and loading on DNA. J Mol Biol **416:** 163-175.

SAKATO, M., Y. ZHOU and M. M. HINGORANI, 2012b ATP binding and hydrolysis-driven rate-determining events in the RFC-catalyzed PCNA clamp loading reaction. J Mol Biol **416:** 176-191.

SCHOFIELD, M. J., and P. HSIEH, 2003 DNA mismatch repair: molecular mechanisms and biological function. Annu Rev Microbiol **57:** 579-608.

SERTIC, S., S. PIZZI, F. LAZZARO, P. PLEVANI and M. MUZI-FALCONI, 2012 NER and DDR: classical music with new instruments. Cell Cycle **11:** 668-674.

SHARMA, V., L. B. COLLINS, T. H. CHEN, N. HERR, S. TAKEDA *et al.*, 2016 Oxidative stress at low levels can induce clustered DNA lesions leading to NHEJ mediated mutations. Oncotarget.

SMITH, A. J., T. E. CAWSTON and B. L. HAZLEMAN, 1985 A rapid and reproducible method for the analysis of immune complexes using affinity chromatography and Western blotting. J Immunol Methods **84:** 125-134.

SULLI, G., R. DI MICCO and F. D'ADDA DI FAGAGNA, 2012 Crosstalk between chromatin state and DNA damage response in cellular senescence and cancer. Nat Rev Cancer **12:** 709-720.

THAM, K. C., R. KANAAR and J. H. LEBBINK, 2016 Mismatch repair and homeologous recombination. DNA Repair (Amst) **38:** 75-83.

TRAVER, S., P. COULOMBE, I. PEIFFER, J.R. HUTCHINS *et al.*, 2015 MCM9 Is Required for Mammalian DNA Mismatch Repair. Mol Cell **59**: 831-839.

TURINETTO, V., and C. GIACHINO, 2015 Multiple facets of histone variant H2AX: a DNA double-strand-break marker with several biological functions. Nucleic Acids Res **43:** 2489-2498.

V, S., R. BHAGAT, S. P. C, R. P. V and L. KRISHNAMOORTHY, 2014 Microsatellite instability, promoter methylation and protein expression of the DNA mismatch repair genes in epithelial ovarian cancer. Genomics **104:** 257-263.

VENDETTI, F. P., A. LAU, S. SCHAMUS, T. P. CONRADS, M. J. O'CONNOR *et al.*, 2015 The orally active and bioavailable ATR kinase inhibitor AZD6738 potentiates the anti-tumor effects of cisplatin to resolve ATM-deficient non-small cell lung cancer in vivo. Oncotarget **6:** 44289-44305.

VRIEND, L. E., R. PRAKASH, C. C. CHEN, F. VANOLI, F. CAVALLO *et al.*, 2016 Distinct genetic control of homologous recombination repair of Cas9-induced double-strand breaks, nicks and paired nicks. Nucleic Acids Res.

VYMETALKOVA, V. P., J. SLYSKOVA, V. KORENKOVA, L. BIELIK, L. LANGEROVA *et al.*, 2014 Molecular characteristics of mismatch repair genes in sporadic colorectal tumors in Czech patients. BMC Med Genet **15:** 17.

WANG, J. C., 2002 Cellular roles of DNA topoisomerases: a molecular perspective. Nat Rev Mol Cell Biol 3: 430-440.

YAN, T., J. E. SCHUPP, H. S. HWANG, M. W. WAGNER, S. E. BERRY *et al.*, 2001 Loss of DNA mismatch repair imparts defective cdc2 signaling and G(2) arrest responses without altering survival after ionizing radiation. Cancer Res 61: 8290-8297.

ZELLER, C., W. DAI, N. L. STEELE, A. SIDDIQ, A. J. WALLEY *et al.*, 2012 Candidate DNA methylation drivers of acquired cisplatin resistance in ovarian cancer identified by methylome and expression profiling. Oncogene 31: 4567-4576.